RESEARCH DEPARTMENT REPORT SERIES no. 8-2009 ISSN 1749-8775

HUNTINGDON CASTLE MOUND, CAMBRIDGESHIRE OSTEOLOGICAL ANALYSIS OF THE HUNTINGDON CASTLE POPULATION

ENVIRONMENTAL STUDIES REPORT

Stefanie Vincent and Simon Mays

ARCHAEOLOGICAL SCIENCE

ENGLISH HERITAGE

Research Department Report Series 8-2009

Simon Mays
Fort Cumberland, Fort Cumberland Road
Eastney, Portsmouth. PO4 9LD

Osteological Analysis of the Huntingdon Castle Population.

S. Vincent and S. Mays

NGR: TM3969580356

ISSN 1749-8775

SUMMARY

Fifty-five inhumations from Huntingdon Castle Mound, Cambridgeshire were examined. The majority of the burials are Anglo-Saxon in date while the remainder are post-medieval. 20 males, 16 females, 6 unsexed adults and 13 juveniles were examined and demographic, metric, non-metric and pathological data is presented. A case of possible treponemal disease dating to 1010-1170 was identified.

ARCHIVE LOCATION

Fort Cumberland, Fort Cumberland Road, Eastney, Portsmouth. PO4 9LD

DATE OF RESEARCH

Research was undertaken in 2008-2009.

CONTACT DETAILS

Fort Cumberland, Fort Cumberland Road, Eastney, Portsmouth. PO4 9LD.
Simon Mays; 02392 856779; Simon.Mays@english-heritage.org.uk.

CONTENTS

Introduction to Huntingdon Castle Mound.

Huntingdon Castle Mound is located in west Cambridgeshire. The area was part of the 'Danelaw' between AD 878-921(Malim, 1998), until the ruling Danish forces were forced out by Edward the Elder. There is documentary evidence that Huntingdon became a focus for skirmishes between the two sides, with both Danish and Saxon fortifications in the area (Hunter Blair, 1956:81, Taylor, 1978:6). The stone castle was erected in the 11th century, by which time Huntingdon had a population of approximately two thousand people (Darby, 1977:5).

The site at Huntingdon Castle Mound was excavated in the winter of 1967 by the Ministry of Public Buildings and Works after human remains were unexpectedly uncovered during construction. No site report has been published and at the current time the site archive cannot be located.

During the excavations the burial ground was provisionally dated to the 9th/10th century. Evidence was also found for Roman occupation of the site, along with the remains of a possible siege tower which was erected during the 1100's. It was also thought that a small number of burials excavated may have been associated with a gallows known to be on the site in the post-medieval period.

A total of 55 inhumations have been identified, however loss of the site archive means that stratagraphic information is absent. A basic plan of the burials has been re-constructed from grid numbers recovered from the packaging of the skeletons (Figure 1). Burial numbers do not run consecutively.

Figure 1: reconstructed site plan of Huntingdon Castle Mound.

	1	2	3	4	5	6
N					55 56	
M					5 30 43	31 35 32 36 44 67 68
L				93 79 102 66	71 72 73 100	1 16 25 3 36 26 17 40 61 60 63 80
K			49 14 88 13 50 84 91 90	82 15 45 86 62 87		
J			20 22 10		6	
I			11			

It is assumed that North is toward the top of the grid. The grid squares are thought to be 50ft (15.24m) square.

Dating

As there were only tentative archaeological dates attached to the skeletal remains an AMS radiocarbon dating program was instigated to establish the period from which the skeletal collection came. Samples from 14 skeletons were submitted for dating; thirteen of these were randomly chosen from across the site while B17a was dated because interesting pathological changes which will be discussed later in the report.

Burial No.	Lab No.	Date range (68% confidence)	Date Range (95% confidence)
B10	SUERC-21104	cal AD 770–880	cal AD 690–890
B17a	SUERC-19641	cal AD 1020–1160	cal AD 1010–1170
B22	OxA-19121	cal AD 1510–1645	cal AD 1470–1650
B30	SUERC-19645	cal AD 1020–1150	cal AD 1010–1160
B31	OxA-19890	cal AD 1030–1160	cal AD 1020–1170
B36	SUERC-21105	cal AD 880–970	cal AD 770–990
B49	OxA-19891	cal AD 1030–1160	cal AD 1020–1170
B56	OxA-19122	cal AD 890–990	cal AD 890–1020
B66	SUERC-21106	cal AD 1210–1270	cal AD 1160–1280
B67	OxA-19892	cal AD 880–970	cal AD 870–990
B80	SUERC-19646	cal AD 770–900	cal AD 720–950
B86	OxA-19220	cal AD 1450–1620	cal AD 1440–1640
	SUERC-19647	(mean)	(mean)
B87	OxA-19893	cal AD 880–970	cal AD 780–990
B100	OxA-19123	cal AD 1020–1160	cal AD 1020–1160

The dating results show that the burial site was in use between the 8th and 17th centuries. At the time of excavation the majority of the burials were believed to be late Saxon and the dating which has been completed so far does not contradict this. There is documentary and archaeological evidence of a post medieval gallows on the site and the radiocarbon results date some of the burials to the post-medieval period. The lack of stratagraphic evidence from the site makes it difficult to ascertain if the burial ground was in continuous use, however it seems likely that the presence of the castle and associated buildings created a hiatus in the use of the cemetery during the later medieval period. As the size of the assemblage is relatively small it was decided to analyse all the burials as one group and it was deemed other late Saxon urban sites were the best comparative material.

Bone preservation and skeletal completeness.

A total of 55 discrete inhumations have been identified. In three cases (B17, B23 and B50) multiple individuals were collected and packaged together under one burial number. This was presumably the result either of multiple individuals being buried in one grave or an inability to distinguish individual grave cuts on site. Two of the burials contained mixed adult and juvenile remains, while the third contained two adults. During analysis the mixed remains were separated and recorded separately; the original burial number was kept and the skeletons allocated an A/B suffix. There was disarticulated bone present in almost every burial and a substantial amount of charnel was recovered. This charnel is recorded only by general context number, indicating that no archaeological evidence of a discreet burial was observed.

Skeletal completeness and bone preservation were estimated by visual assessment. The level of bone preservation was scored as; good, moderate or poor, while completeness was the estimated percentage of skeletal elements present.

Table 1: Preservation and completeness of burials.

Completeness	Preservation.			Total
	Good	Moderate	Poor	
<20%	5	2	1	8
20-40%	7	7	1	15
40-60%	11	2	2	15
60-80%	5	1	0	6
+80%	11	0	0	11
Total	39	12	4	55

Preservation levels were high among the group, with 70.9% of burials falling into the 'good' category. Plotting preservation status on the burial plan reveals no clustering of preservation levels. Juvenile burials are not less well preserved than adults.

Completeness of the burials ranges widely, but 67% of burials have less than 60% of the skeleton represented. Unfortunately the lack of site archive means interpretating the disturbance of the burials is difficult. Incompleteness may be due to intercutting of burials or truncation of graves by later structures, but without site plans this is impossible to substantiate. Alternately the interruption of the burials could be the result of modern interference; newspaper reports of the period make it clear that disturbance to the remains occurred both as a consequence of construction and looting of the site by members of the public. These factors together could account for some of the loss of bone.

In addition to the estimates of skeletal completeness, individual elements were recorded and the tables below show the representation of the individual elements recovered.

Table 2: representation of skeletal elements (all skeletons).

Skeletal element	No. present
Crania	27
Mandibles	17
Cervical vertebrae	137
Thoracic vertebrae	368
Lumbar vertebrae	185
L ribs	260
R ribs	267
Sterna	39
L Claviclae	27
R Claviclae	27
L Scapulae	30
R Scapulae	30
L Humeri	34
R Humeri	34
L Radii	37
R Radii	34
L Ulnae	35
R Ulnae	32
L carpals	52
R carpals	35
L metacarpals	110
R metacarpals	79
L hand phalanges	18
R hand phalanges	14
Unsided hand phalanges	187
L Pelves	42
R Pelves	44
L Femora	40
R Femora	40
L Patellae	7
R Patellae	14
L Tibiae	34
R Tibiae	38
L Fibulae	27
R Fibulae	26
L Calcanei	22
R Calcanei	17
L Tali	17
R Tali	17
L tarsals*	27
R tarsals*	36
L metatarsals	63
R metatarsals	70
L foot phalanges	3
R foot phalanges	8
Unsided foot phalanges	19

Table 3: representation of skeletal elements (adult burials).

Skeletal element	No. present
Crania	20
Mandibles	13
Cervical vertebrae	105
Thoracic vertebrae	286
Lumbar vertebrae	145
L ribs	201
R ribs	188
Sterna	21
L Claviclae	22
R Claviclae	19
L Scapulae	24
R Scapulae	21
L Humeri	26
R Humeri	26
L Radii	27
R Radii	25
L Ulnae	25
R Ulnae	22
L carpals	43
R carpals	26
L metacarpals	83
R metacarpals	62
L hand phalanges	16
R hand phalanges	13
Unsided hand phalanges	137
L Pelves	33
R Pelves	33
L Femora	31
R Femora	30
L Patellae	7
R Patellae	13
L Tibiae	27
R Tibiae	31
L Fibulae	20
R Fibulae	20
L Calcanei	16
R Calcanei	15
L Tali	14
R Tali	15
L tarsals*	26
R tarsals*	34
L metatarsals	54
R metatarsals	59
L foot phalanges	3
R foot phalanges	8
Unsided foot phalanges	17

* excluding calcanei and tali.

Demographic composition of the Huntingdon Castle burials.

Adult sex was determined using cranial and pelvic morphology (White and Folkens, 2005). In older juveniles with fused acetabula, pelvic morphology was also applied. As is standard practise, no attempt was made to sex younger juveniles.

Juvenile aging was primarily estimated using tooth formation (Mays, 1998; Gustafson and Koch, 1974 [reproduced in Hillson, 1996, pg 135]). Where dentition was absent age was estimated by epiphyseal fusion (Mays, 1998; Scheuer and Black, 2000) and comparison of long bone length with juveniles from a contemporary site who could be aged by tooth development (Mays, 2007). Foetal and neonatal age was estimated from long-bone length using the regression equations of Scheuer *et al* (1980). Adult age was primarily estimated using molar wear (Brothwell, 1981); unfortunately the size of the sample proved too small to calibrate tooth wear from juveniles. Pubic symphisis morphology (Suchey *et al*, 1986, 1988) was used as a supplementary technique and where dentition was absent or incomplete.

Demography.

Table 4: demographic breakdown of the adult population.

	Adult age ranges				
	18-29	30-49	50+	Adult	Totals
Male	3	5	4	6	18
Probable Male			1	1	2
Female	2	3	2	8	15
Probable Female				1	1
Unsexed	1			5	6
Total	6	8	7	21	42

NB: from now on probable males/females will be included in male/female categories.

Plotting sex data on the burial plan reveals no sex divisions in the cemetery. The even ratio of males:females in the cemetery mirrors the patterns seen at other late Saxon sites and is expected in a cemetery serving the general population:

	Male	Female
Huntingdon	20	16
Caister-on Sea	49	50
North Elmham	82	76
School Street, Ipswich	28	35
Norwich Castle	39	22

50% of the Huntingdon Castle assemblage did not have the skeletal elements present needed to assign age to an individual and comparing the age at death distribution with other contemporary sites is impractical.

Table 5: demographic breakdown of the juvenile population.

	Juvenile age ranges				
	0-4	5-8	9-14	15-18	Totals
Male	0	0	0	0	0
Probable Male	0	0	1	1	2
Female	0	0	0	0	0
Probable Female	0	0	0	0	0
Unsexed	4	2	3	2	11
Total	4	2	4	3	13

The range for juvenile age is 42 weeks in utero – 17 years. A comparison of the age at death distribution of the Huntingdon Castle population with that of the School Street population (Mays, 1989) shows that both sites had a fairly even distribution of juveniles across the four categories displayed above. The late Saxon sites of North Elmham (Wells, 1980) Caister-on-Sea (Anderson, 1993) and Norwich Castle (Stirland, 1985) all record peaks in the number of children dying in specific age groups and it may be that the small number of individuals represented at Huntingdon Castle has masked any such peak in this material.

Metric variation

Stature

Adult stature was estimated using Trotter and Gleser (1958, in Brothwell, 1981, pg 100). The formulas are sex specific, so no stature information could be gained from the burials which were unsexed.

Table 6: distribution of adult stature (cm).

	154-160	≤ 160-165	≤ 165-172	≤ 172-180	≤ 180-185
Male	1	1	7	8	1
Female	9	3	-	1	-

Table 7: range and mean of adult stature (cm).

	No.	Stature Range	Mean Stature
Male	18	160.8-184.4	171.5
Female	13	154.4-174.3	160

Comparison of stature between the population of Huntingdon Castle and other late Saxon groups shows that the Huntingdon adults were of a fairly average stature, although the height range of the Huntingdon females is slightly higher than their contemporaries:

Table 8: comparative stature of Huntingdon adults (cm).

	Male Stature		Female Stature	
	Average	Range	Average	Range
Huntingdon	171.5	160.8-184.4	160	154.4-174.3
Caister-on Sea	170.8	157-185.8	161.1	148.6-172.3
North Elmham	172.1	162.3-180.7	157.4	142.4-169.7
School Street, Ipswich	171.5	163-186	159.1	149-172
Norwich Castle	170.1	159.4-179.2	160.1	156.2-165.2

Cranial measurements

Measurements were taken as outlined in Brothwell (1981) with additional measurements taken from Howells (1973). Of the forty-two adults in the Huntingdon group only twenty had crania present; of these only two are complete. This limits the data available for cranial measurements. The results are shown in appendix 2.

Cranial index

Cranial index was calculated as in Brothwell (1981). Only eight individuals had crania complete enough to allow the correct measurements to be taken.

Table 9: cranial indices by sex

	No.	Mean	SD	Range
Male	5	74.1	3.69	71.6-76.5
Female	3	76.3	1.54	75.0-78.5

Table 10: cranial indices by category

	Dolichocephalic	Mesocephalic	Brachycephalic	Hyperbrachycephalic
Male	4	1	0	0
Female	0	3	0	0

The cranial indices of the Huntingdon Castle population indicate that the cranial shape tended to be long and narrow. This shape is typical of the Anglo-Saxon period and is comparable with the cranial indices found at North Elmham (Wells, 1980), Caister-on-Sea (Anderson, 1993) and Norwich Castle (Stirland, 1985).

Meric and cnemic indices

Meric and cnemic indices gauge the cross-sectional shape of the femur and tibia respectively. Differences in cross-sections between populations are thought to be caused by mechanical adaptation and as such may indicate the range of physical activity of the individual (Brothwell, 1981).

Table 11: meric indices

	Meric index L				Meric index R			
	No.	Mean	s.d.	Range	No.	Mean	s.d.	Range
Male	12	81.7	8.3	63.1-97.0	12	82.6	6.3	74.7-95.0
Female	10	78.5	6.1	70.9-86.7	10	82.4	7.7	71.9-93.7
Unsexed	1	78.3	-	78.3	1	78.3	-	78.3

Table 12: cnemic indices

	Cnemic index L				Cnemic index R			
	No.	Mean	s.d.	Range	No.	Mean	s.d.	Range
Male	11	69.2	5.7	61.7-79.4	11	70.6	5.5	61.6-80
Female	10	70.4	13.4	33.2-83.1	9	76	5.0	68-82.3
Unsexed	2	70	4.5	65.5-74.5	3	71.6	4.6	66-71.1

Non-metric variation

Non-metric variations are a range of minor variations in presence or morphology of structures such as foramina or facets. While it has been established that some traits (such as the Inca bone) have a genetic component, the causes of the majority of the traits are unknown. Both cranial and post-cranial non-metric variations were recorded. The post-cranial traits were taken from Finnegan (1978) and the cranial traits from Berry and Berry (1967). Some traits are known to manifest in childhood, only to disappear in adulthood; for this reason only adult results are reported here.

Table 13: frequency of cranial non-metric traits in adults.

Trait	1	0	1/1	-/1	1/-	1/0	0/1	-/0	0/-	0/0
Metopic suture	1	13								
Ossicle at lambda	1	12								
Lambdoid ossicle	6	4								
Inca Bone	0	13								
Sagittal ossicle	0	6								
Ossicle at bregma	0	11								
Coronal ossicle	2	7								
Fronto-temporal articulation			0	0	0	0	0	2	2	1
Epipteric bone			0	1	0	0	0	1	2	2
Squamo-parietal ossicle			0	0	0	0	0	2	2	3
Parietal notch bone			0	0	0	0	1	2	1	5
Auditory torus			0	0	0	0	0	3	3	11
Foramen of Hushke			0	0	0	1	1	2	4	8
Ossicle at asterion			0	0	0	2	0	1	1	5
Clinoid bridging			0	0	0	0	0	1	0	2
Pterygoid bridging			0	0	0	0	0	1	0	4
Palatine torus	1	8								
Maxilla torus	0	8								
Mastoid foramen extra-sutural			3	0	1	0	0	2	1	2
Mastoid foramen absent			1	0	0	1	0	2	1	3
Double condylar facet on occipital			0	0	0	0	0	1	2	8
Parietal foramen			4	0	1	1	2	0	0	5
Accessory infra-orbital foramen			2	0	0	1	0	1	1	5
Zygomatic facial foramen			4	5	2	0	0	0	2	2
Divided hypoglossal canal			1	0	1	0	1	1	1	5
Post condylar canal patent			1	0	0	1	2	1	1	3
Pre-condylar tubercle			0	0	1	0	0	1	0	8
Foramen ovale incomplete			0	0	0	0	0	2	0	7
Accessory lesser palatine foramen			1	1	0	0	1	0	0	5
Supra-orbital foramen complete			1	1	0	1	0	0	3	5
Maxillary M3 absent			0	0	0	0	0	0	0	9
Mandibular M3 absent			2	0	0	0	0	0	0	10
Mandibular torus	0	9								
Mylohyoid bridging			1	0	0	0	0	2	0	8

Table 14: frequency of post-cranial non-metric traits in adults.

Trait	1	0	1/1	-/1	1/-	1/0	0/1	-/0	0/-	0/0
Fossa of Allen			5	0	2	2	0	4	3	15
Poirers facet			1	0	0	0	1	3	6	20
Plaque formation			8	1	2	0	1	3	3	13
Exostosis in trochantric fossa			6	1	5	2	1	1	3	9
Supra-condylar process			0	1	0	1	0	5	10	15
Septal apature			0	1	1	0	1	2	9	13
Acetabular crease			4	0	0	1	0	1	5	16
Accessory sacral facets			6	1	0	2	0	3	4	11
Spinabifida occulta	0	27								
Six sacral segments present	10	17								
Acromial articular facet			0	0	0	0	0	1	5	7
Os acromale			0	0	0	1	0	1	6	6
Supra-scapular foramen			0	0	0	0	0	2	4	4
Vastus notch			2	0	0	0	0	6	1	4
Vastus fossa			0	0	0	0	0	6	1	5
Emarginate patella			0	0	0	0	0	6	1	5
Lateral squatting facets			1	0	0	0	0	4	4	13
Medial squatting facets			5	1	3	2	2	4	0	4
Anterior calcaneal facet double			3	2	1	0	0	2	2	8
Anterior calcaneal facet absent			0	0	0	0	0	4	3	11
Atlas facet double			2	0	1	0	0	0	1	14
Posterior atlas bridging			0	0	0	1	1	0	1	14
Lateral atlas bridging			0	0	0	1	1	0	2	13

Key: 1=trait present, 0=trait absent, - element not present for observation. Bilateral traits are scored left/right.

There is a high prevalence of the occurrence of six sacral segments, 37% in the twenty seven individuals with sacra available for examination. Increases in the total number of vertebrae present are not uncommon and occur most frequently in the lumbar and sacral vertebra (Barnes, 1994:78). The additional vertebrae begin to form at week two, but it is not yet known if genetic or environmental factors are the cause (Usher and Nørregaard Christensen, 2000). This is a higher frequency than is seen in the School Street (11.1%) and North Elmham (4.7%) populations. Plotting the occurrences of a sixth sacral segment on the burial plan reveals no clustering indicative of familial groups and it may be that the shared genetic inheritance of the group or a specific environmental factor they were exposed to caused the high prevalence of the trait.

Different sternal morphologies result from variation in the timing of fusion of the sternal segment (Barnes, 1994:219). There were 21 adults with sterna available for examination and of these 17 have type one sterna. Three individuals have normal type two sterna (Barnes, 1994:219) while a fourth individual with a type two sternum exhibits marked medio-lateral widening at segments 3-4, with a corresponding circular depression on the plural side of the sternum, suggestive of a delay in fusion between the segments (Barnes, 1994:218).

Four individuals exhibit cranial shifts of the vertebral borders while one exhibits a caudal shift. Variations around the borders of regional vertebra are common and result in the vertebrae above or below the border taking on characteristics of the vertebra in the neighbouring region (Barnes, 1994: 79). There are two cases of cleft posterior arch of the atlas, caused by a developmental delay in formation of the two halves of the arch (Barnes, 1994: 119). It is estimated that about 5% of the modern adult population have clefting of the atlas arch; in life the gap is bridged by a fibrous band which mimics the missing bony segment (Barnes, 1994:120).

Oral Pathology.

Caries.

Dental caries (or cavities) occur when the acid by-product of bacteria in dental plaque causes focal destruction of the tooth (Hillson, 1996:269). Dental caries were scored as present or absent.

Table 15: prevalence of caries in adult population.

	Individuals scored for caries	Individuals with caries
Male	10	4
Female	3	3
Unsexed	1	1
Totals	14	8

Table 16: Prevalence of caries by tooth in adults.

Maxillary

	LM3	LM2	LM1	LPM2	LPM1	LC	LI2	LI1	RI1	RI2	RC	RPM1	RPM2	RM1	RM2	RM3	Total
Teeth Present	5	6	4	6	7	7	5	4	5	7	8	10	9	7	7	6	103
Carious teeth	1	1	0	1	1	0	0	0	0	0	0	0	0	1	1	0	6
Teeth present	3	7	6	10	9	7	8	8	7	7	8	11	10	7	8	3	119
Carious teeth	1	0	1	1	1	0	0	0	0	0	0	1	1	0	0	0	6

Mandibular

	% Caries by Individual	% Caries by tooth.
Huntingdon Castle	57	5.4
Caister-on-sea		1.8
North Elham	-	6.4
School Street, Ipswich	44.6	10
Norwich Castle	-	2.6

The data shown above demonstrates that the frequency of caries by tooth in the Huntingdon Castle population falls in the middle of contemporary sites while the rate of caries by individual is significantly higher. This may point to low levels of oral hygiene in the Huntingdon Population but it is worth noting that a significant number of the adult population of Huntingdon Castle did not have dentition available for examination.

Ante-mortem tooth loss.

Ante-mortem tooth loss was scored as present or absent in individuals where one or more tooth sockets could be examined. The results are shown below;

Table 17: adult tooth loss.

	Individuals scored for tooth loss	Individuals with tooth loss.
Male	10	6
Female	4	3
Unsexed	1	1
Totals	15	10

Table 18: results by tooth of ante-mortem loss.

Maxillary

	LM3	LM2	LM1	LPM2	LPM1	LC	LI2	LI1	RI1	RI2	RC	RPM1	RPM2	RM1	RM2	RM3	Total
Sockets Present	8	10	9	10	10	10	10	11	13	13	13	13	13	12	11	9	175
Tooth Loss	0	3	4	3	2	2	2	2	2	2	2	2	3	4	3	1	37
Sockets present	7	12	12	12	12	12	12	11	11	11	11	11	11	11	11	7	174
Tooth Loss	3	4	5	0	0	0	1	2	1	1	0	0	0	3	3	4	27

Mandibular

Ante-mortem tooth loss is known to be age related, with older individuals showing a higher rate of loss than younger people. The most common causes of tooth loss are caries and periodontal disease, although it can also result from traumatic injury (Moore and Corbett, 1971).

	% Ante-mortem tooth loss by individual.	% Ante-mortem tooth loss by tooth socket.
Huntingdon Castle	66.7	18.3
North Elmham	-	11.1
School Street, Ipswich	47.6	10.5
Norwich Castle	-	4

The frequency of ante-mortem tooth loss at Huntingdon Castle is considerably higher than those reported at other comparable sites. Again it is worth noting that only a small percentage of the population had dentition available for study.

Periapical Voids

Periapical voids have commonly been referred to in the literature as abscesses, granulomas or cysts. Recent work has highlighted the tendency to apply such terms generically to any void found associated with a tooth and advocates that more precision

be taken in identifying such voids, so their effect on the individual can be better represented (Ogden, 2008).

The presence of periapical voids were recorded for all teeth and tooth sockets available for examination. One periapical void was found in the juvenile population at a first right mandibular incisor. Adult results are shown below;

Table 19: periapical voids in adults.

	Individuals scored for periapical voids	Individuals with periapical voids
Male	10	4
Female	4	3
Unsexed	1	0
Totals	15	7

Table 20: periapical voids by tooth.

Maxillary

	LM3	LM2	LM1	LPM2	LPM1	LC	LI2	LI1	RI1	RI2	RC	RPM1	RPM2	RM1	RM2	RM3	Total
Sockets Present	8	10	9	10	10	10	10	11	13	13	13	13	13	12	11	9	175
Periapical Voids	1	0	1	0	0	0	0	0	0	0	0	2	2	1	0	0	7
Sockets present	7	12	12	12	12	12	12	11	11	11	11	11	11	11	11	7	174
Periapical Voids	0	0	1	0	0	1	0	0	0	0	1	0	0	2	0	0	5

Mandibular

46.6% (7/15) of the adults scored were found to have periapical voids, with a frequency of 3.4% (12/349) for all sockets scored. Using the criteria laid out by Ogden (2008) further diagnosis of the periapical voids in the Huntingdon population was attempted. Four periapical voids were found to be granulomas, while a fifth was thought to be either a granuloma or a cyst. The cause of the remaining periapical voids could not be identified.

Calculus.

Calculus is caused by the mineralization of dental plaque and is indicative of low oral hygiene (Hillson, 1996:255). Supra-gingiveal calculus was scored using the criteria of Dobney and Brothwell (1987). The results are shown below;

Table 21: calculus in adults.

	Grade 0	Grade 1	Grade 2	Grade 3	Grade 4	Total
Male	2	4	4	1	0	11
Female	0	2	0	1	0	3
Unsexed	0	0	0	0	0	0
Totals	2	6	4	2	0	14

The results show that 85% of adults with dentition had calculus deposits, however it should be noted that of forty two adults in the population only fourteen had dentition present to score.

Linear Enamel Hypoplasia

Linear enamel Hypoplasias (LEH) are transverse bands of deficient enamel thickness on the crown of the tooth, which develop during crown formation. They occur as a result of stress upon the growing individual and have been linked to disease and malnutrition (Hillson, 1996:165). LEH were systematically recorded in the anterior dentition and noted when they occurred elsewhere. In the anterior dentition the presence, tooth affected and distance of the defect from the cemento-enamel junction (CEJ) were recorded;

Table 22: LEH by individual.

	Number of defects per individual		
	0	1	2
Male	7	2	1
Female	3	0	1
Total	10	2	2

In the Huntingdon population there were six linear enamel hypoplasias found in four individuals (HC022, HC030, HC066 and HC091). Of these six, four occurred in the anterior dentition while two were found on the pre-molars.

Where LEH occurred in the anterior dentition an attempt was made to estimate the age at which the defect arose. Unfortunately the incomplete nature of the assemblage meant there were not enough teeth to calibrate tooth formation scales as described by Reid and Dean (2000). Instead where the teeth effected with LEH were unworn the tooth height was measured and the age at which the LEH occurred was calculated. In cases where wear had occurred to the tooth exhibiting LEH, an estimation was made as to which fifth of the tooth the defect occurred in and age of occurrence was estimated using the results of Reid and Dean (2000).

Table 23: defects of anterior dentition.

Burial	Tooth	Distance of LEH from CEJ	Tooth height	Estimated age of occurrence
HC091	C_R	11.1	13.4	1.7-2
HC022	$I1_R$ $I1_L$	7.0 6.5	Unknown	1.3-1.7
HC030	$I1^R$	4	Unknown	2.9-3.9

N.B. Measurements are in mm and age is in years.

HC066 was found to have two LEH's on $1PM_R$ and it was estimated that these occurred between two and four years of age.

In addition to the occurrence of LEH, one example of a major enamel disruption in the rear dental arcade was found. HC091 has a systematically recorded LEH on C_R, along with enamel disturbance on the $PM2_R$ and $M1_R$. The $M1_R$ has grossly disturbed cuspal architecture and a dramatic enamel hypoplasia on the buccal side of the tooth, leaving a gap of approximately 2mm between the edge of the buccal enamel and the occlusal surface of the tooth (Plate 1). The occlusal surface itself shows enamel disruption in the form of multiple small pits across its surface. The $PM2_R$ also exhibits an abnormality in cusp formation and has an LEH extending part-way across its buccal surface. There are also pit form enamel hypoplasias across the buccal surface of the tooth (Ogden, 2008). Mulberry molars as a result of congenital syphilis can cause a change in cuspal architecture with accompanying disruption of tooth enamel, however the changes observed here do not fit the criteria set out by Hillson (1998). The enamel disruption of the first molar and second premolar, coupled with the alteration in cusp organisation are consistent with a condition termed cuspal enamel hypoplasia (Ogden et al, 2007). Using tooth formation charts (Mays, 1998) it has been estimated that the disturbance to $M1_R$ occurred within the first 1.5 years of life, while the LEH and associated pitting on the pre-molar occurred at between 2-3.5years of age. This combined with the LEH of the right mandibular canine suggests that multiple episodes of stress were placed upon the individual.

Joint disease.

Osteoarthritis.

Osteoarthritis (OA) is degeneration of the joint surfaces causing osteophytosis of joint margins, surface porosity and eburnation. OA occurrence is known to increase with age and is thought in part, to be a result of mechanical loading stresses on joints (Rogers and Waldron, 1995).

The severity of OA was scored using a system adapted from Sager (1969; reproduced in Brothwell, 1981):

Grade 0 Normal bone surface
Grade 1 Intermittent osteophytes
Grade 2 Surface porosity; may be accompanied by osteophytes
Grade 3 Eburnation; may be accompanied by porosity and osteophytes

Table 24: maximum OA score in individual adults from Huntingdon.

	OA grade.			
	Grade 0	Grade 1	Grade 2	Grade3
Male	6	5	2	7
Female	2	3	5	6
Unsexed	3	1	1	1
Total	11	9	8	14

Table 25: distribution of osteoarthritis in adults at Huntingdon.

	Grade			
Skeletal element	0	1	2	3
L mandibular condyle	5	0	0	2
R mandibular condyle	7	0	0	0
Cervical vertebrae	62	15	8	14
Thoracic vertebrae	197	17	20	8
Lumbar vertebrae	102	15	10	3
L ribs	149	30	20	2
R ribs	135	32	15	6
L medial clavicle	20	0	1	0
R medial clavicle	14	0	2	0
L lateral clavicle	10	0	5	0
R lateral clavicle	8	0	5	0
L glenoid fossa	18	2	0	0
R glenoid fossa	16	3	0	1
L proximal humerus	20	0	0	0
R proximal humerus	15	0	0	0
L distal humerus	21	0	0	1
R distal humerus	17	2	0	0

L proximal radius	18	1	0	1
R proximal radius	19	0	0	0
L distal radius	20	0	0	1
R distal radius	21	0	0	0
L proximal ulna	17	3	0	0
R proximal ulna	15	3	0	0
L distal ulna	20	0	0	0
R distal ulna	14	1	0	0
L carpals	43	0	0	0
R carpals	26	0	0	0
L metacarpals	81	1	0	1
R metacarpals	62	0	0	0
L hand phalanges	16	0	0	0
R hand phalanges	13	0	0	0
Unsided hand phalanges	136	0	0	1
L acetabulum	25	0	0	1
R acetabulum	26	0	0	0
L proximal femur	28	0	0	1
R proximal femur	28	0	0	0
L distal femur	21	4	0	0
R distal femur	21	3	0	1
L patella	7	0	0	0
R patella	10	3	0	0
L proximal tibia	24	0	0	0
R proximal tibia	28	1	0	0
L distal tibia	19	0	0	0
R distal tibia	24	0	0	0
L proximal fibula	13	0	0	0
R proximal fibula	12	0	0	0
L distal fibula	14	0	0	0
R distal fibula	13	0	0	0
L calcaneus	16	0	0	0
R calcaneus	15	0	0	0
L talus	14	0	0	0
R talus	15	0	0	0
L tarsals*	26	0	0	0
R tarsals*	34	0	0	0
L metatarsals	53	0	0	1
R metatarsals	59	0	0	0
L foot phalanges	3	0	0	0
R foot phalanges	8	0	0	0
Unsided foot phalanges	17	0	0	0

*excluding tali and cancanei

There is no significant difference in the frequency, severity or location of OA occurrence between sexes.

Degenerative disc disease.

Osteoarthritis of the vertebral facet joints were scored as detailed previously. The non-synovial joints between vertebral bodies degenerate in a different way: long term mechanical stress in the vertebral column can cause degeneration of the intervertebral disc. This can lead to spreading of the disc surface and production of osteophytes and porosity on the vertebral body surfaces (Rogers and Waldron, 1995).

The recording of osteophytosis in the Huntingdon population was adapted from Sager (1969), reproduced in Brothwell (1981):

Grade 0 Normal bone surface
Grade 1 Osteophytes
Grade 2 Surface porosity covering less than half of the vertebral surface
Grade 3 Surface porosity coving more than half of the vertebral surface.

Table 26: maximum grades of degenerative disc disease by individual.

	Maximum grade			
	0	1	2	3
Males	7	3	5	2
Females	4	5	4	2
Unsexed	1	1	0	0
Total adults	12	9	9	4

Note: For inclusion, individuals needed to show at least one vertebral body present for observation

Table 27: prevalence of degenerative disc disease by vertebrae.

	Cervical				Thoracic				Lumbar			
	0	1	2	3	0	1	2	3	0	1	2	3
Males	25	4	4	8	77	39	6	0	38	21	8	0
Females	25	7	3	5	50	31	15	0	26	23	9	1
Unsexed	0	0	0	0	7	7	0	0	0	0	0	0
Total adults	50	11	7	13	134	77	21	0	64	44	17	1

There are no significant differences in the frequency of degenerative disc disease between males and females. In both sexes the lumbar vertebrae are the most commonly involved in degenerative disc disease, followed by the thoracic and cervical regions of the spine.

Diffuse Idiopathic Skeletal Hyperostosis (DISH).

DISH in skeletal remains is characterised by vertebral ligamentous ossification leading to ankylosis (Rogers and Waldron, 2005). The cause of the condition is not fully understood but links have been made to diabetes, obesity and metabolic disturbances (Rogers and Waldron, 2001; Mays, 2000), whilst a clinical study of Finnish populations found geographical differences in DISH prevalence rates (Julkunen et al, 1971). Studies have shown that the prevalence of DISH is higher in males than females and increases with age

(Julkunen et al, 1971). DISH was diagnosed when two complete bony bridges between vertebrae were present (Julkunen et al, 1971) and differentiated from other arthropathies using the criteria set down by Rogers and Waldron (1995).

There was one case of DISH found in the Huntingdon Castle population, in a male aged 50+ (HC061). There is ankylosis of the vertebral bodies of C6/C7/T1, T6/T7 and further interlocking, non-ankylosing ossifications between T5/T6, T7/T8/T9, L2/L3. There is ossification of both acetabular labra, both glenoid labra, at the site of the Achilles tendon insertion on the left calcaneus and at the site of the insertion of the quadriceps tendon on the right patella.

Hallux Valgus.

Hallux valgus is the lateral deviation of the first toe, instigated by biomechanical forces on the foot, usually from footwear. It is commonly associated with bunion formation at the metatarso-phalangeal joint and osteoarthritic changes at the metatarsal head (Mays, 2005a).

One individual was found to be suffering from hallux valgus. HC003 is an unsexed adult exhibiting bilateral hallux valgus, indicating that the individual wore restrictive footwear. The level of skeletal completeness means that the frequency of the condition could have been underestimated in the population: of the forty-two adults examined only thirteen have one or more metatarsal present for examination.

Trauma.

Fractures.

There was a prevalence of fractures of 21% with respect to the total number of adults examined; no evidence of fracture was found in the juvenile material. Twenty three fractures occur in nine adults, all post-cranial. Rib fractures are the most common type of fracture, accounting for 65% (15/23) of fractures found, with the majority of these fractures (11/15) occurring in one individual (HC030). This pattern follows that seen by Roberts and Cox (2003:206;239); in their review of medieval skeletal material rib fractures were the most frequent fracture observed.

HC011 (male, 50+) has a compression fracture of the left superior facet of the atlas; the facet height has been reduced in comparison to the right and new bone formation is present along the lateral edge of the facet (Plates 2 and 3). The other cervical vertebrae exhibit osteoarthritic changes, possibly as a secondary reaction to the fracture. The likely aetiology for the fracture is a compressive force to the skull and neck, perhaps as a result of a fall (Resnick and Niwayama,1988:2932).

HC072 (unsexed, adult) has a healed avulsion fracture effecting the anterior body of T3 (Plates 4 and 5), probably caused by hyperextension of the spine (Resnick and Niwayama, 1988:2940).

In HC093 (female, 50+) C3 and C4 have become ankylosed at their bodies and right facet joints. C3 is laterally deviated to the right and there is no retention of intervetebral disk space (Plate 6). Large non-ankylosing osteophytes have formed at the vertebral bodies and right facet joints of C4, C5, and C6. There is a smooth walled concave depression on the right hand side of the bodies of C3 and C4, suggestive of an aneurism of the vertebral artery. The lateral displacement of C3 suggests the ankylosis is secondary to a subluxation of the cervical spine (Resnick and Niwayama, 1988:2937).

HC050 (male, 50+) has spondylolysis of L2, L3 and L6. The condition is a cleft in the pars interarticulars of the vertebrae. In this individual bi-lateral spondylolysis has led to the separation of the posterior section of the neural arch from the rest of the vertebra. It is believed that spondylolysis is caused by a fatigue fracture but the exact nature of the stress which causes the condition has not yet been determined. Spondylolithisis is a related condition caused by bi-lateral spondylolysis which results in anterior slippage of the vertebral body, which results in doming of vertebral body below. The body of S1 is domed in individual HC050 suggesting that spondylolisthesis of L5 has occurred (Mays, 2006).

There is one example of hand trauma in the collection; HC066 (male, 35-45) exhibits a Bennett fracture of the first right metacarpal. Bennett fractures are fractures involving the

articular surface of the thumb, usually caused by striking the thumb against a hard surface with force (Peterson and Bancroft, 2006).

The right ilium of HC066 (male, 35-45) has been fractured and a portion of the bone has become displaced. The displaced bone has healed leaving perforations through the iliac crest (Plate 7). The injury is well healed with no evidence of infection in the surrounding bone. The origin of the trauma is most likely a direct downward blow to the iliac crest.

HC093 (female, 50+) has a fracture of the right femoral neck with secondary damage to the right acetabulum. The fracture has shortened the femoral neck and inferiorly displaced the femur head. The superior edge of the right acetabular rim has suffered a height loss of approx 5mm and has a ragged appearance. This lesion is suggestive of hip trauma in which a lateral impact forced the femur head against the acetabulum. The loss of acetabular rim height may suggest a minor fracture occurred during the incident but the ragged nature of the surface is more consistent with the fragmentation of the rim edge. This can occur when a tear in the articular cartalidge at the base of the acetabular labrum permits ingress of synovial fluid into the subchondral bone. This can result in the reabsorbition of multiple areas of subchondral bone, undermining the acetabular rim until it can no longer sustain the mechanical forces at the hip and fragments (Mays, 2005b).

Two individuals have healed fibula fractures in their distal diaphyses (HC014 and HC079). Both fibulae fractures are oblique indicating an indirect trauma and their position on the fibulae is indicative of a lateral rotative force (such as a twist of the ankle) being the fracture mechanism (Lovell, 1997). The right tibia of HC079 has remodelled periosteal bone formation at the same level as the fibula fracture, indicating inflammation or infection of the surrounding soft tissue may have occurred at the time of the fracture. Lovell (1997) notes that fractures involving the ankle are the second most frequent fracture to occur in modern populations.

HC080 has a linear fracture of the first left metatarsal which runs anterior-posterior from the head to the base (Plate 8). The linear nature of the fracture suggests it was caused by an impact to the distal end of the first toe.

Weapon-related injury

Burial HC073 (male, 25-35) has an unhealed edged weapon wound on the cranium (Plate 9). There is a linear cut on the left parietal bone measuring 37.3mm by 1.7mm, which is restricted to the outer table of the cranium. The right edge of the depression is straight while the left edge shows flaking of the bone. There are no fractures of the skull around the wound, indicating a sharp bladed instrument caused the injury (Lovell, 1997). The lack of healing at the site indicated the injury occurred peri-mortem. Demographically males are more likely to be injured by physical aggression, with the frontal and left parietals being the most frequent areas for injuries to occur (Roberts and Manchester, 2005:109).

Schmorl's nodes.

Schmorl's nodes are pressure defects on the vertebral surface, caused by herniated material from the intervertebral disc exerting pressure on the surface of the vertebral body (Rogers and Waldron, 1995). In dry bone they present as indentations in the vertebral surface. The primary cause of Schmorl's nodes is greatly debated; while it seems that trauma (either repeated micro-trauma or a major traumatic event) is the direct cause of the defect, there may be underlying genetic or developmental factors which pre-dispose some individuals to the development of Schmorl's nodes (Resnick and Niwayama, 1988:1527). Research into Schmorl's nodes as a cause of pain is ongoing and recent papers seem to suggest that chronic pain can accompany the lesions, although further research is needed to quantify this (Faccia and Williams, 2008).

Table 28: distribution of Schmorl's nodes by vertebra.

	Cervical Vertebrae			Thoracic Vertebrae			Lumbar Vertebrae		
	Total Verts	Verts with nodes	No. of Nodes	Total Verts	Verts with nodes	No. of Nodes	Total Verts	Verts with nodes	No. of Nodes
Male	41	0	0	122	36	46	67	2	3
Female	40	0	0	106	17	21	63	8	8
Unsexed	0	0	0	14	5	5	0	0	0
Total	81	0	0	242	58	72	130	10	11

Table 29: results of Schmorl's nodes by individual.

	Individuals without nodes	Individuals with nodes
Male	6	11
Female	10	5
Unsexed	1	1
Total	17	17

NB: For inclusion, individuals needed to show at least one vertebral body present for observation

There is no significant difference between the frequency of Schmorl's nodes in males and females. The distribution of Schmorl's nodes within the spine is the same for males and females; the thoracic vertebrae are most often effected, followed by the lumbar spine. No Schmorl's nodes were present in the cervical vertebrae.

Supra-acetabular cysts.

Supra-acetabular cysts are cavities within the iliac bone which communicate with the cortical surface of the bone at or around the acetabular rim. The cysts are caused by ingress of synovial fluid into the subchondrial bone via tears in the acetabular labrum or neighbouring cartilage (Mays, 2005b).

Four individuals from Huntingdon Castle have supra-acatabular cysts; HC025, HC066, HC093 and HC102. HC093 (female, 50+) has supra-acetabular cysts and a fracture of

the acetabular rim in association with a fracture to the femur neck, as discussed above. The rim of the left acetabulum of HC025 (male, adult) has a ragged appearance, suggesting the rim has fragmented. This is caused by the formation of several supra-acetabular cysts, which undermine the edge of the rim leading to its collapse (Mays, 2005b). The remaining individuals have bilateral supra-acetabular cysts, with no observable trauma of the acetabular bone.

Osteochondritis Dissecans.

Osteochondritis dissecans is the detachment of a small segment of bone from an articular surface, following necrosis brought on by repeated micro-trauma. The appearance of the lesion in dry bone is a small missing section of cortical bone, leaving an irregular surface with clearly de-lineated edges (Auferheide and Rodriguez-Martín, 1998:81).

There are two probable cases of osteochondritis dissecans in the Huntingdon population. The first is HC043, an adult female with the condition in the capitulum and trochlear notch of the right elbow. The second is HC090 an adult male with osteochondritis dissecans of the lateral condyle of the left distal femur. The knee and the elbow are respectively, the first and third most common sites of osteochondritis dissecans occurrence in modern populations (Auferheide and Rodríguez-Martin, 1998:82-83).

Traumatic Myositis Ossificans.

Traumatic myositis ossificans occurs when an injury to tendinous, ligamentous or muscle attachments results in a haematoma which subsequently ossifies (Resnick and Niwayama, 1988:4247). It should be noted that not all trauma of this type will lead to ossification of the haematomas and so the level of trauma to tendinous, ligamentous and muscle attachments in a population will be underestimated in the skeletal remains.

There are two cases of traumatic myositis ossificans in the Huntingdon population; HC030 (male, 50+) displays an ossification at the distal diaphysis of the right tibia and fibula, suggestive of an injury to the interosseous ligament. HC031 (female, adult) displays ossification at the lesser trochanter of the right femur indicating a tear of the psoas major and/or Iliacus muscle.

Third Intercondylar Tubercle of Parsons.

The third intercondylar tubercle of Parsons (TITP) has been linked to injury of the anterior cruciate ligament (Mays and Cooper, In press). TITP is found in four individuals; two cases are bi-lateral, one is unilateral and the fourth has only one tibia available for study. Three of the effected individuals are female, while the fourth is unsexed. The potential for the Parsons' tubercle to be used as an indicator of activity has been noted,

however further work is needed in this area before such definitive links can be made (Mays and Cooper, In press).

Porotic Hyperostosis.

Porotic hyperostosis is most commonly a result of iron deficiency anaemia. The causes of the iron deficiency are complex and only rarely represent dietary deficiency; instead factors affecting the uptake of iron into the body (parasite load, pregnancy, blood loss etc) are the main causes (Stuart-Macadam, 1992). Cribra orbitalia, a category of porotic hyperostosis presents as small perforations in the roof of the orbits. Cribra orbitalia was scored as either porotic or cribrotic in line with Brothwell (1981).

Table 30: occurrence of cribra orbitalia by individual.

	Absent	Porotic	Cribrotic
Male	3	3	0
Female	4	0	0
Total adults	7	3	0
Juvenile	0	0	0

NB: For inclusion individuals needed one or both orbits present for examination.

There were only a small number of individuals in the Huntingdon population with one or both orbits present, making comparisons with other sites impractical. No cases of porotic hyperostosis affecting the skull vault were found.

Infectious disease.

Treponemal disease.

There are three types of treponematosis which effect the skeleton; syphilis (congenital and acquired), yaws and bejel (also known as endemic syphilis). Yaws is found only in tropical climates, while today bejel is most commonly found in hot, dry areas (such as the Middle east and Africa). Archaeological evidence of bejel has been found in Northern European populations; the disease is transmitted via contact with the open sores of infected individuals. In modern populations syphilis is found world-wide (Ortner, 2003:274). There is one possible case of treponemal disease present in the Huntingdon Castle population.

HC017 is an adult female whose skeleton is represented only from the lumbar vertebrae downwards. Both tibiae and the left fibula (right is not present) show concentric thickening throughout their diaphysis. The majority of the bone deposits are smooth and well remodelled but there are some areas which have a fine grained appearance, suggesting lesions active at the time of death. Both tibiae have small plaques of bone with undercut edges. A post depositional break on the distal diaphysis of the left tibia shows that the medullary cavity has become occluded with trabecular bone. Radiographic analysis shows the medullary cavities of all three bones are completely occluded with cancellous bone. The distal halves of the diaphysis of both femora appear concentrically thickened and there are well remodelled areas of bone formation on the posterior side of the distal diaphysis of both bones. Radiographic analysis shows the medullary cavity has become occluded in both femora (Plates 10-13).

The radiographic findings exclude Paget's disease of bone as a cause of the pathological changes. There is no sinus formation to indicate the presence of pyogenic osteomyelitis and the absence of lytic lesions rule out fungal infections as a cause. The concentric thickening of the leg bones, the presence of small undercut plaques in the subperiosteal new bone deposits and occlusion of the medullary canal suggest treponemal disease as the cause of the pathological changes (Ortner, 2003:286).

As yaws is found only in tropical climates it may be discounted as a cause of the pathology seen here. One of the main distinguishing factors between bejel and syphilis is that the destruction of the nasal area and hard palate seen in syphilis only rarely occur in bejel (Ortner, 2003:278), however as the skull is not present in this case it is not possible to distinguish between bejel and syphilis.

Tuberculosis.

Tuberculosis is a chronic infectious disease chiefly caused by *Mycobacterium bovis* and *Mycobacterium tuberculosis*. Transmission is via droplet formation and *Mycobacterium bovis* can also be transmitted to humans from cattle through the ingestion of infected dairy products (Ortner, 2003:227).

HC036 exhibits extensive pathological changes to the right hip joint. The femoral head and neck have been completely resorbed, the lesser trochanter is present but has lost its rounded shape and become flattened. The greater trochanter is missing but post-depositional damage at the site make it impossible to ascertain the mechanism of the loss. The right femur is significantly thinner and lighter than the left femur. A small section of the acetabular rim can still be identified but the majority is obscured by new bone formation, which has completely filled the acetabulum. The edges of the lesion are partially remodelled but the centre appears to have been active at the time of death. The right innominate bone is lighter and thinner than the left and the superior and inferior pubic ramus have an elongated appearance. The loss of the articular surfaces of the femur and acetabulum have caused eburnation in the area where the two bones have made contact (Plate 14).

Hip dislocations (both traumatic and congenital) produce a faux joint surface, which is not seen here and can be excluded as a cause of the pathology. More probable is tuberculosis effecting the hip joint, causing destruction of the surface of both femur and acetabular surfaces. The unilateral appearance of the lesion is consistent with tuberculosis and the hip joint is the second most common area for skeletal lesions of tuberculosis to occur (Aufderheide and Rodriguez-Martin, 1998:139).

Non- specific infection.

When the infective agent causing pathological changes cannot be identified it is termed a non-specific infection. The majority of non-specific infections in the Huntingdon population are periostitis; changes to the surface of a bone in repose to inflammation of the overlying soft tissue (Ortner, 2003:206).

Table 31: showing cases of periostisis by individual.

Burial	Location	Type of lesion
HC017b	Pleural surface of right rib fragment	Unremodelled
HC032	The entirety of the plural surfaces of 11 left and 10 right ribs, inferior half of plural surface of sternal body.	Unremodelled
HC032	Diaphysis of right tibia and fibula	Remodelled
HC061	Endocranial surface to right of bregma (post-depositional damage makes the extent of the lesion unidentifiable	Unremodelled
HC072	Distal metaphysis of right radius	Unremodelled and remodelled
HC080	Diaphysis of right tibia and fibula	Remodelled
HC084	Diaphysis on the tibiae	Remodelled and partially remodelled
HC091	Diaphysis on the tibiae	Remodelled

The extensive woven bone formation confined on the pleural surface of the ribcage of individual HC032 is suggestive of a pulmonary infection. Tuberculosis is the disease most likely to cause lesions on the ribs and these lesions are most likely to be distributed bilaterally as seen here. However while it is possible that tuberculosis was responsible for the infection seen here, rib lesions are not pathognomonic of a specific infection, rather they are only indicative of pulmonary disease (Roberts and Lucy 1994, Mays *et al* 2002).

Four individuals have non-specific infectious changes on their lower leg bones. The lower leg bones are a common site for the occurrence of periostitis in archaeological remains. While the exact reason for this is unknown the close proximity of the tibia to the surface of the skin is a possible explanation; this position leaves the bone more susceptible to trauma which can introduce infectious agents into the soft tissue around the bone (Ortner, 2003:209).

Two individuals exhibit non-specific infections which are not solely periosteal in nature. HC031 (a female adult) and HC066 (a male, 35-45) exhibit near identical concentric fusiform swellings on the distal diaphyses of their femora (Plates 15-17). In HC031 the lesion occurs on the right femur, while in HC066 the lesion is on the left femur. In both cases the swelling is concentrated on the posterior of the diaphysis at the junction of the supracondylar lines. The surfaces of the lesions are raised and roughened cortical bone; radiographic analysis show that in both cases the medullary canal has been occluded by cancellous bone. Of HC031's lower leg bones only the proximal thirds are present and show remodelled bone formation on both tibiae and fibulae in addition to a partially remodelled focal periosteal lesion on the lateral side of the left tibia. HC066 has post depositional damage to both tibiae and the left fibula (right is absent), there is a small area

of roughened, well remodelled bone deposition on the lateral side of the proximal diaphysis of the left tibia. It is considered probable that the lesions on the femora and lower leg bones share a common cause, however diagnoses are considered which take into account the possibility that the femoral lesions occurred separately from the lower leg lesions. Paget's disease of bone can be excluded as the characteristic radiographic appearance is absent, as is the sinus formation of pyogenic osteomylitis. Two diagnoses which fit the pathological changes are sclerosing osetomyelitis of Garré and treponemal disease. Sclerosing osetomyelitis of Garré is a rare disease which causes a sclerotic and fusiform thickening of the bone. This thickening can lead to narrowing of the medullary cavity. The disease frequently effects only one bone and is often limited to one side of the diaphysis (Auferheide and Rodriguez-Martín, 1998:178). Treponemal disease may cause periosteal bone response with a roughened outer surface, effecting only part of a bone. The medullary cavity can become narrowed and in later stages totally obscured by sclerotic trabeculae (Ortner, 2003:273-297). Diagnosis is made difficult in this case as taken in isolation the pathological changes in the femur are consistant with both sclerosing osteomyelitis of Garré and a treponemal infection. When the two cases are viewed together however the rare occurrence of sclerosing osteomyelitis of Garré and the lesions which occur in both individuals in bones other than the femur indicate early stage treponemal disease is the more likely cause of the lesions.

Neoplasms.

Tumours are the result of uncontrolled tissue proliferation and can be either benign or malignant. Tumours which remain localised are said to be benign; however these growths can still cause problems by interfering with the functions of other parts of the body through their sheer size. Tumours which contain several cell types and grow unchecked are considered malignant and can metastasise to secondary locations (Ortner, 2003:503). Three individuals from Huntingdon exhibit neoplastic changes.

HC061, a male aged 50+ has a single osteoma on the medial surface of the right side of the mandible. Osteomas are benign neoplasms, most commonly found on the cranial vault (Ortner, 2003:506), but known to appear elsewhere (Mays, 2007, Steinbock, 1976:327).

HC049 is an adult male. The cortical surfaces of the left femur (of which only the distal half is present), the medial surface of the tibiae, the right femur and the right fibula (the left is absent) are covered in finely pitted lesions (Plate 18). In places this appears to be pitting of the original cortical surface but slight new bone formation is present at others. Approximately 75% of the way up the left femur, the bone shaft terminates in an area of ante-mortem destruction. The cortical walls of the diaphysis at this end are internally bevelled and have a rather rough and somewhat porous appearance. The sub-periosteal surface at the edge of this lesion has partially remodelled bone deposits (Plate 19). The extent of the lytic lesion on the femur is impossible to judge due to post depositional damage, but the femur head and greater trochanter are present, indicating some proximal parts of the femur were spared destruction.

The fine pitting of cortical surfaces coupled with focal destruction of the cortex from within, is typical of metastatic carcinoma. The primary sites of neoplastic involvement most likely to develop skeletal metastases are the breast, kidney, lung, thyroid and prostate (Resnick & Niwayama, 1988:388). The prostate produces metastases which are predominantly blastic, unlike those seen here and the sex of the individual makes breast cancer unlikely. Solitary, slow growing lytic defects in long-bone shafts are most frequently caused by renal or thyroid carcinomas and so both are possible candidates for the primary focus in the current case (Ortner, 2003: 535). However as the distribution of skeletal lesions is not predicted by the primary carcinoma no definitive diagnosis can be made (Ortner, 2003:539).

HC084 is a male aged 17-23 years. Post depositional damage to the frontal bone superior to the left orbit reveals replacement of diploë with abnormal nodular bone with large lytic void spaces. The surface of the abnormal bone is irregular and fine grained. The lesion extends to the adjoining surface of the greater wing of the sphenoid and medially to the rostrum of the sphenoid body, although post depositional damage makes

it impossible to precisely gauge the extent of the lesion. There is superficial erosion of the left orbital roof and the bone there has a fine grained appearance. There is a small pitted area on the outer surface of the frontal bone, over the abnormal diploë (Plates 20 - 22). The lesion presents a mottled appearance radiographically. This is a predominantly blastic lesion originating in either the diploë or inner table of the skull. The fine grained appearance of the bone is suggestive of actively expanding bone at the time of death but the dense nature of the bone when radiographed suggests a slow growing lesion. The lesion has the appearance of a neoplasm and there are several possible differential diagnoses.

The frontal and parietal bones are common sites for the development of an haemangioma (Steinbock, 1976: 351). However haemangioma are lytic in nature, frequently producing a 'sunburst' effect on radiographs when present in the skull (Ortner, 2003: 513), at variance with what is observed here. Fibrous dysplasia causes the enlargement of bone by the erosion of the original cortex which is then replaced with sclerotic trabecular bone. However the gross enlargement of the bone accompanied by a thinning of cortical bone characteristic of fibrous dysplasia are not seen in this case. Osteosarcoma is a primary malignant tumour of bone which usually occurs in those under twenty-five. The tumour is highly variable in morphology, but it is rarely found in the skull and the current case lacks the 'sunburst' appearance that is often associated with this type of tumour on X-ray (Ortner, 2003: 524). Meningiomas originate in the meningial tissue and erode through the endocranial surface often eliciting a bony reaction. They are slow growing, producing heavily ossified and well-ordered bone formation. The average age of onset for meningioma is >45 years and a recent study found that 96% of suffers were over thirty (Anderson, 1992). Of the above diagnoses, meningioma or osteosarcoma are the most likely options, although a definitive conclusion cannot be reached.

Miscellaneous conditions.

Burial HC093 exhibits a teardrop enlargement of the middle nasal concha, the surface of which is covered in tiny spicules of bone. The enlargement measures 20mm anterior-posterior and 15mm medio-laterally, with the largest anterior-posterior measurement occurring inferiorly. The nasal septum deviates left so its lateral surface almost makes contact with the adjacent surface of the maxilla (Plate 23). Radiographic analysis shows no abnormality of the internal structure of the enlarged concha and there is no indication that the growth is neoplastic in origin. Clinical texts note that swelling of the nasal conchae is a common occurrence in modern populations, which can have several aetiologies including chronic rhinitis (Berger and Glass, 2006). Symptoms can range from the non-existent through to mild headaches and nasal obstruction (Berger and Gass, 2006; Kunachak, 2002).

Burial HC102 (male, 22-43), exhibits bilateral ankylosis of the sacroiliac joints (sij), via bony bridges at the superior margins. The joint space is preserved and post depositional damage at the right sij shows that the joint surfaces are normal. There is no evidence of erosive joint lesions in the skeleton although much of the vertebral column and many of the hand and foot bones are missing. The rest of the skeleton does not exhibit bone formation due to DISH or sub-clinical DISH. The positioning of the bridging at the sij is suggestive of idiopathic fusion as described by Dar et al (2005). That study notes that the condition is more frequent in males and that frequency increases with age.

HC035 has symmetrical deposits of woven bone formation on the posterior diaphysial surface of the left and right humeri, the diaphysis and distal metaphysis of both radii, the distal anterior metaphysis of both ulnae, the lateral side of the diaphysis of both femora (with the bone formation most pronounced at the linea aspera), the anterior of the distal metaphysis of both femora, the diaphyses of both tibiae (with the bone formation being most pronounced at the soleal line) and the diaphysis of the left fibula (the right fibula is absent). These pathological changes are consistent with a diagnosis of hypertrophic osteoarthopathy. The disease manifests with symmetrical deposits of sub-periosteal new bone formation. Tubular bones (especially those distal to the elbow and knee) are most often effected and the lesions are more prominent around areas of musculo-tendinous attachments. In modern populations inter-thoracic cancer or chronic chest infections are the most common causes of hypertrophic osteoarthopathy, although the mechanism of the bony lesions is not yet fully understood (Mays and Taylor, 2002).

Summary.

A total of fifty five discrete inhumations were analysed from Huntingdon Castle mound. The majority of skeletons are well preserved but most burials were incomplete. Archaeological evidence suggested the majority of the inhumations were of later Anglo-Saxon date, with the possibility of some later burials associated with a post-medieval gallows. It was thought probable that no burials took place at the site during the intervening years due to the proximity of the castle buildings. Radiocarbon dating has confirmed the presence of Anglo-Saxon and post-medieval burials. Demographic analysis of the site established the presence of 20 males, 16 females, 6 unsexed adults and 13 juveniles. Plotting sex data on a basic reconstructed burial plan revealed no clustering of burials. The roughly 50:50 sex split is matched in other Anglo-Saxon cemeteries from the region. The incomplete nature of many of the burials means that a large proportion of the adult burials could not be aged and it was considered impractical to compare age at death distribution with other sites. The juvenile age at death distribution does not identify any high risk ages.

Analysis of the pathology in the Huntingdon population show that most of the traumatic injuries suffered most likely resulted from common everyday accidents. The blade injury on the cranium of individual HC073 is the only evidence of inter-personal violence in the population. The most interesting pathology found in the collection is the case of probable treponematosis effecting HC017a. Discussion as to the origin of treponemal disease is still ongoing, with evidence being presented for both New and Old World origins for the disease. Radiocarbon dating places this burial firmly in the pre-Columbian period, adding to the weight of evidence suggesting the presence of treponematosis outside of the Americas before they were visited by Columbus. To date this is one of the earliest cases of the disease found in Britain.

References

Anderson, S 1993 'The Human Skeletal Remains from Caister-on-Sea' In *Caister-on-Sea Excavations by Charles green, 1951-55* By Darling, M J East Anglian Archaeology, Report No. 60 Norfolk: Norfolk Museums Service

Anderson, T 1992 'A Medieval Example of Meningiomatous Hyperostosis' *Journal of Palaeopathology* 4 (3) 141-154

Aufderheide, A C and Rodríguez-Martín, C 1998 *The Cambridge Encyclopaedia of Human Palaeopathology* Cambridge: Cambridge University Press

Barnes, E 1994 *Developmental Defects of the Axial Skeleton in Palaeopathology* Colorado: University Press of Colorado

Berger, G and Gass, S 2006 'The Histopathology of the Hypertrophic Inferior Turbinate' *Archives of Otolaryngology-head and Neck Surgery* 132, 588-94

Berry, A C and Berry, R J 1967 'Epigenetic Variation in the Human Cranium' *Journal of Anatomy* 101 (2), 361-79

Brothwell, D 1981 *Digging up Bones* 3rd ed Oxford: Oxford University Press

Dar, G , Peleg, S , Masharawi, Y , Steinberg, N , Rothschild, B M , Peled, N , Hershkovitz, I 2005 'Sacroiliac Joint Bridging: Demographical and Anatomical Aspects' *SPINE* 30 (15), 429-32

Darby, H C 1977 *Medieval Cambridgeshire* Cambridge: The Olender Press

Dobney, K and Brothwell, D 1987 'A Method for Evaluating the Amount of Dental Calculus on Teeth from Archaeological Sites' *Journal of Archaeological Science* 14, 343-51

Duhig, C 1998 'The Human Skeletal Material' *The Anglo-Saxon Cemetery at Edix Hill (Barrington A), Cambridgeshire* Eds T Malim and J Hines York Council for British Archaeology 112

Faccia, K J and Williams, R C 2008 'Schmorl's Nodes: Clinical Significance and Implications for the Bioarchaeological Record' *International Journal of Osteoarchaeology* 18, 28-44

Finnegan, M 1978 'Non-metric Variation of the Infracranial Skeleton' *Journal of Anatomy* 125, 23-37

Hillson, S 1996 *Dental Anthropology* Cambridge: Cambridge University Press

Hillson, S Grigson, C Bond, S 1998 'Dental Defects of Congenital Syphilis' *American Journal of Physical Anthropology* **107**, 25-40

Howells, W W 1973 'Cranial Variation in Man: A Study by Multivariate Analysis of Patterns of Difference Among Recent Human Populations' *Papers of the Peabody Museum of Archaeology and Ethnography* No. **67**

Hunter Blair, P 1956 *An Introduction to Anglo-Saxon England* Cambridge: Cambridge University Press

Julkunen, H, Heinonen, O P and Pyörälä, K 1971 'Hyperostosis of the spine in an adult population' *Annals of the Rheumatic Diseases* **30**, 605-12

Kunachak, S 2002 'Middle Turbinate Lateralization: A Simple Treatment for Rhinologic Headache' *The Larygoscope* **112**, 870-72

Lovell, N C, 1997 'Trauma analysis in Palaeopathology' *Yearbook of Physical Anthropology* **40**, 139-70

Malin, T 1998 'Chapter one: Background to the Excavations' *The Anglo-Saxon Cemetery at Edix Hill (Barrington A), Cambridgeshire* Eds T Malim and J Hines York Council for British Archaeology **112**

Mann, R W and Murphy, S P 1990 *Regional Atlas of Bone Disease: A Guide to Pathological and Normal Variation in the Human Skeleton* Springfield, Illinois: Charles C Thomas

Mays, S 1998 *The Archaeology of Human Bones* London: Routledge

Mays, S 2000 'Diffuse Idiopathic Skeletal Hyperostosis (DISH) in Skeletons from Two Medieval English Cemeteries' *Journal of Palaeopathology* **12 (1)**, 25-36

Mays, S , Fysh, E , and Taylor, G M 2002 'Investigation of the link between visceral surface rib lesions and Tuberculosis in a Medieval Skeletal Series from England Using Ancient DNA' *American Journal of Physical Anthropology* **119**, 27-36

Mays, S 2005a 'Paleopathological study of Hallux Valgus' *American Journal of Physical Anthropology* **123**, 139-49

Mays, S 2005b 'Supra-acetabular Cysts in a Medieval Skeletal Population' *International Journal of Osteoarchaeology* **15**, 233-46

Mays, S 2006 'Spondylolysis, Spondylolisthesis and Lumbo-sacral Morphology in a Medieval English Skeletal Population' *American Journal of Physical Anthropology* **131**, 352-62

Mays, S 2007 'Part three: the human remains' In *Wharram: A study of settlement on the Yorkshire Wolds, XI; The Churchyard* Eds Clark, E and Wrathnell, S Exeter: Short Run Press Limited

Mays, S and Cooper, L A 'Palaeopathological investigation of the third intercondylar tubercle of Parsons' *International Journal of Osteoarchaeology In press*

Mays, S and Taylor, G M 2002 'Osteological and Biomolecular Study of Two Possible Cases of Hypertrophic Osteoarthropathy from Mediaeval England' *Journal of Archaeological Science* **29**, 1267-1276

Moore, W J and Corbett, M E 1971 'The Distribution of Caries in Ancient British Populations: 1 Anglo-Saxon Period' *Caries Research* **5**, 151-168

Moore, W J and Corbett, M E 1973 'The Distribution of Caries in Ancient British Populations: 2 Iron Age, Romano-British and Mediaeval Periods' *Caries Research* **7**, 139-153

Ogden, A R, Pinhasi, R, White, W J 2007 'Gross Enamel Hypoplasia in Molars From Subadults in a 16th-18th Century London Graveyard' *American Journal of Physical Anthropology* **133**, 957-66

Ogden, A 2008 'Advances in the Palaeopathology of Teeth and Jaws' In: Pinhasi and Mays, eds *Advances in Human Palaeopathology* Chichester: John Wiley & Sons 283-307

Ortner, D J 2003 *Identification of Pathological Conditions in Human Skeletal Remains* London: Academic Press

Peterson, J J and Bancroft, L W 2006 'Injuries in the fingers and thumb of the athlete' *Clinics in Sports Medicine* **25**, 527-42

Reid, D J and Dean, M C 2000 'Brief Communications: The Timing of Linear Hypoplasias on Human Anterior Teeth' *American Journal of Physical Anthropology* **113**, 135-39

Resnick, D and Niwayama, G 1988 *Diagnosis of Bone and Joint Disorders* 2nd ed USA: W B Saunders Company,

Roberts, C A and Lucy, D 1994 'Inflammatory Lesions of Ribs: An Analysis of the Terry Collection' *American Journal of Physical Anthropology* **95**, 169-182

Roberts, C A and Cox, M 2003 *Health and disease in Britain; from Prehistory to the Present Day* Gloucestershire: Sutton Publishing,

Roberts, C A and Manchester, K 2005 *The Archaeology of Disease* 3rd ed Gloucestershire: Sutton Publishing,

Rogers, J and Waldron, T 1995 *A Field Guide to Joint Disease in Archaeology* England: John Wiley & Sons Ltd

Rogers, J and Waldron, T 2001 'DISH and the Monastic Way of Life' *International Journal of Osteoarchaeology* 11, 357-65

Scheuer, J L, Musgrave, J H, Evans, S P 1980 'The estimation of late fetal and perinatal age from limb bone length by linear and logarithmic regression' *Journals of Human Biology* 7 (3), 257-65

Scheuer, J L and Black, S 2000 *Developmental Juvenile Osteology* Great Britain: Elsivier Academic Press

Steinbock, R T 1976 *Palaeopathological Diagnosis and Interpretation* Springfield: Charles C Thomas

Stirland, A 1985 'Chapter 6: The Human Bones' In *Excavations within the North-East Bailey of Norwich Castle, 1979* Ed Ayers, B East Anglian Archaeology, Report No 28 Norwich: Norfolk Archaeological Unit

Stuart-Macadam, P 1992 'Porotic Hyperostosis: A New Perspective' *American Journal of Physical Anthropology* 87, 39-47

Suchey, J M and Katz, D 1986 *Skeletal age standards derived from an extensive multi-racial sample of modern Americans; instructional materials accompanying the male pubic symphiseal models* Distributed by France Casting; Fort Collins; Colorado

Suchey, J M, Brooks, S T, Katz, D 1988 *Instructional materials accompanying the female pubic symphiseal models of the Suchey-Brooks system* Distributed by France Casting; Fort Collins; Colorado

Taylor, A 1978 *Anglo-Saxon Cambridgeshire* Cambridge: Cambridge University Press

Usher, Bethany M, and Nørregaard Christensen, Mette 2000 'A sequential Developmental Field Defect of the Vertebrae, Ribs and Sternum in a Young Woman of the 12th Century AD' *American Journal of Physical Anthropology* 11, 355-67

Wells, C 1980 'The Human Bones' In *Excavations in North Elham Park vol 1* Ed Wade-Martins, P East Anglian Archaeology, Report No 9 Norfolk: Norfolk Archaeological Unit

White, T and Folkens, P 2005 *The Human Bone Manual* Burlington, USA: Elsevier

Plates.

Plate 1; cuspal hypoplasia HC091.

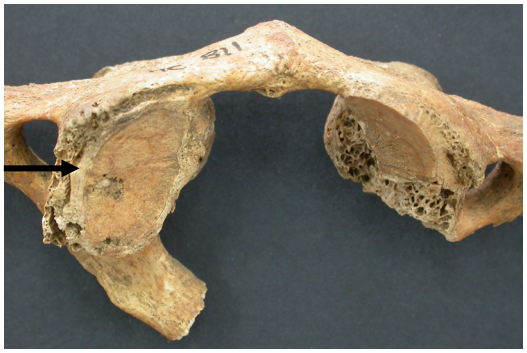

Plate 2; compression fracture of atlas (superior view) HC011.

Plate 3; compression fracture of atlas (posterior view) HC011.

Plate 4; avulsion fracture of a thoracic vertebra (superior view) HC072.

Plate 5; avulsion fracture of a thoracic vertebra (lateral view) HC072

Plate 6; ankylosis of C3 & C4 with lateral/posterior displacement of C3.

Plate 7; fracture of the right iliac crest HC066.

Plate 8; first metatarsal fracture HC080

Plate 9; small unhealed blade wound to left parietal HC073.

Plate 10; pathological changes on tibiae (anterior view) of HC017.

Plate 11; pathological changes on tibiae (medial view) of HC017.

Plate 12; undercut plaque of bone on the left fibula of HC017.

Plate 13; radiograph of tibiae of HC017.

Plate 14; tubercular destruction of the right hip of HC036.

Plate 15; pathological swelling on left femur of HC031.

Plate 16; pathological swelling on femur of HC066

Plate 17; comparison of pathological lesions on the femora of HC031 (top) and HC066 (bottom).

Plate 18; finely pitted lesion on cortex of a long bone HC049.

Plate 19; inner cortex of left femur, showing bevelled edges of lytic lesion HC049.

Plate 20; pathological trabecular bone behind left orbit of HC084.

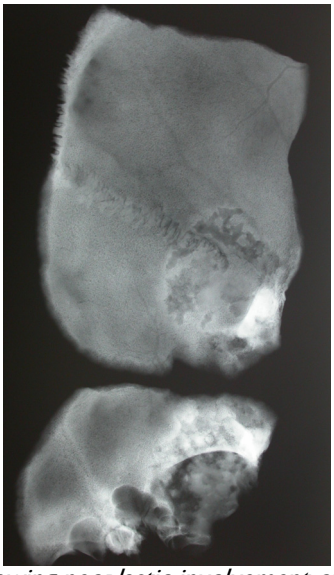

Plate 21; radiograph showing neoplastic involvement of the cranium of HC084.

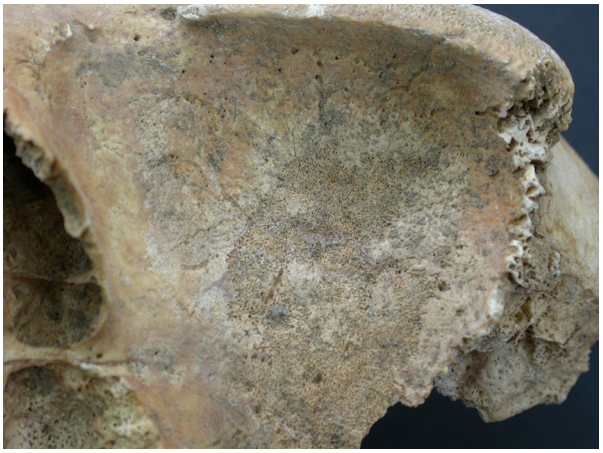

Plate 22; lesion in left orbit of HC084

Plate 23; enlarged right middle nasal concha HC093.

Catalogue of Burials.

Skeleton	Sex	Age	Stature	Preservation	Completeness	C14 Date (95% confidence)
HC001	F	21-53	156.3	G	80+	
HC003	U	ADULT		G	20-40	
HC005	J	9-10		G	40-60	
HC006	?M	14-16		G	40-60	
HC010	M	25-43	174.1	G	40-60	AD 690-890
HC011	M	50+	175.5	G	20-40	
HC013	F	ADULT	157.1	M	20-40	
HC014	F	ADULT	163.5	G	80+	
HC015	U	ADULT		P	<20	
HC016	J	11		G	40-60	
HC017	F	ADULT	158.8	M	20-40	AD 1010-1170
HC017B	J	7-13		M	20-40	
HC020	J	5-6		G	60-80	
HC022	F	19-25	154.7	G	80+	AD 1470-1650
HC023A	U	ADULT		G	<20	
HC023B	F	ADULT		G	<20	
HC025	M	ADULT	174.3	M	40-60	
HC026	J	13-17		P	40-60	
HC030	M	50+	166.1	G	80+	AD 1010-1160
HC031	F	ADULT	162.3	G	20-40	AD 1020-1170
HC032	?M	13-14		G	60-80	
HC035	F	ADULT	163.8	G	40-60	
HC036	F?	ADULT	159.7	G	40-60	
HC038	U	ADULT		G	<20	
HC040	F	ADULT		M	20-40	
HC043	F	ADULT	174.3	G	60-80	
HC044	U	17-25		M	20-40	
HC045	J	2-4		G	40-60	
HC049	M	ADULT	166.6	G	40-60	AD 1020-1170
HC050	F	21-46		M	<20	
HC050B	J	3-4		G	80+	
HC055	M	ADULT	170.6	M	20-40	
HC056	F	25-35	154.4	P	20-40	AD 890-1020
HC060	J	8		G	80+	
HC061	M	50+	160.8	G	80+	
HC062	F	35-45	160.6	G	80+	
HC063	J	42-43 WI		M	<20	
HC066	M	35-45	179.7	G	80+	AD 1160-1280
HC067	M	ADULT	167.0	G	40-60	
HC068	M	40+		G	60-80	
HC071	M	19-25	171.5	G	80+	
HC072	U	ADULT		G	20-40	
HC073	M	25-35	175.0	G	20-40	
HC079	M	ADULT	184.4	G	40-60	
HC080	M	35-50	172.9	M	60-80	AD 720-950

Skeleton	Sex	Age	Stature	Preservation	Completeness	C14 Date (95% confidence)
HC082	J	8-9MNTHS		M	40-60	
HC084	M	17-23	168.9	G	80+	
HC086	J	14-19		G	20-40	AD 1440-1640
HC087	M?	ADULT	167.3	P	40-60	AD 780-990
HC088	F	20-23	156.1	G	20-40	
HC090	M	22-43	177.1	G	<20	
HC091	M	18-19	161.7	G	40-60	
HC093	F	50+	158.3	G	60-80	
HC100	M	ADULT	174.3	M	20-40	AD 1020-1160
HC102	M?	22-43		G	<20	

Appendix 1: notes on individual burials.

HC001

The right transverse processes of S1 and S2 are reduced in height, causing the sacral table to incline to the right. This defect is probably developmental in origin (Barnes, 1994:50).

HC003

The right fourth metatarsal has a smooth plaque of bone on the medial side of the shaft.

Both first metatarsals show lateral deviation of their heads and a large exostosis at the medial epicondyle. This suggests hallux valgus; the lateral deviation of the first toe caused by pressure placed on the foot by shoes (Mays, 2005a).

HC006

There is a benign cortical defect on both femora at the insertion site of the gluteus maximus. Benign cortical defects are common in sub-adults and are usually erased during the growth process (Mann and Murphy, 1990:85).

HC010

There is a small nodule of bone on the proximal metaphysis of the left fibula.

On the left clavicle the attachment site for the costoclavicular ligament is much deeper and wider than that on the right clavicle.

HC011

There is partial non-union of the mendosa suture of the skull on the left hand side.

The facet at the head of the first right rib is absent. The facet on the right of the vertebral body of T1 is normal in appearance,

The left superior facet of the atlas is orientated more horizontally than the right facet, lowering the superior/inferior facet height by 2mm in comparison to the right side of the atlas. There is remodelled new bone formation along the lateral edge of the left facet. Nine of the thirteen vertebrae present have osteoarthritic changes, while all the vertebrae present showed osteophytosis to some degree. There is a non-ankylosing ligamentous ossification running from the occipital to the atlas. The morphology of the injury to the atlas facet indicates a crushing fracture as the most likely cause (Resnick and Niwayama,

1988:2932) and it is possible the other spinal pathology could be a secondary response to the injury.

HC013

The lateral ends of both transverse processes of T12 are present as separate ossicles.

HC014

There is a sternal aperture.

The manubrium and body of the sternum are united. This is probably a developmental anomaly (Barnes, 1994:211).

Three united rib fractures are present in three un-sided fragments; two are at the sternal end of the rib while the third fragment is too small for the location of the fracture to be determined.

The left innominate shows ossification of the acetabular labrum.

The left fibula has a healed, oblique fracture in the distal diaphysis.

Both transverse foramina on C5 are divided, as are the right transverse foramina on C6 and C7.

Type one cervical ribs have formed at C7, indicating a cranial shift at the cervicothoracic border (Barnes, 1994:100).

HC015

The right tibia displays a Parsons tubercle on its proximal articular surface (Mays and Cooper, In press). The left tibia is normal.

HC017

Both tibiae and the left fibula (right is not present) show concentric thickening throughout their diaphysis. The majority of the bone deposits have a smooth well remodelled appearance but there are some areas which have a fine grained appearance, suggesting lesions active at the time of death. Both tibiae show have small plaques of bone with undercut edges. A post depositional break on the distal diaphysis of the left tibia shows that the medullary cavity has become occluded with trabecular bone. Radiographic analysis shows the medullary cavities of all three bones are completely occluded with cancellous bone.

The distal halves of the diaphysis of both femora appear concentrically thickened and there are well remodelled areas of bone formation on the posterior side of the distal diaphysis of both bones. Radiographic analysis shows the medullary cavity has become occluded in both femora. The radiographic findings exclude Paget's disease of bone as a cause of the pathological changes. There is no sinus formation to indicate the presence of pyogenic osteomyelitis and the absence of lytic lesions rule out fungal infections as a cause. The concentric thickening of the leg bones, the presence of small undercut plaques in the subperiosteal new bone deposits and occlusion of the medullary canal suggest treponemal disease as the cause of the pathological changes (Ortner, 2003:283).

HC017b

There is woven bone formation on the internal surface of a right rib fragment. No other ribs are effected.

HC022

There is a frontal foramen present on the right side of the frontal bone and the foramen ovale of the sphenoid is double.

Type 2 cervical ribs have formed at C7 indicating a cranial shift has occurred at the cervicothoracic border (Barnes, 1994:100).

HC023B

There is a ligamentous ossification extending from the posterior border of the inferior facet of the left iliac auricular surface. The corresponding area of the sacrum is absent.

HC025

There are two supra-acetabular cysts (Mays, 2005b) close to the left acetabular rim and the superior edge of the left acetabular rim has a ragged appearance. The ragged appearance of the acetabular rim is consistent with the fragmentation of the edge after ingress of synovial joint fluid, due to damage of the acetabulum labrum and/or the adjacent articular cartilage (Mays, 2005b).

There is ossification of the right acetabular labrum.

HC030

There are six lumbar vertebra present. L2, L3 and L6 have spondylolysis and the body of S1 is domed. Doming of the sacral table has been linked to the development of spondylolisthesis (Mays, 2006).

There are eleven rib fractures effecting the left hand side of the rib cage;

Rib No.	Number of fractures.	Fracture Location
Left 7	2	Posterior angle; sternal end
Left 8	3	Posterior angle; midshaft; sternal end.
Left 9	3	Posterior angle; midshaft; sternal end.
Left 10	2	Posterior angle; sternal end
Left 11	1	Posterior angle

The five fractures which occur at the posterior angle of the ribs are united, but woven bone formation here indicates healing was still underway at time of death. The six remaining fractures are well remodelled, indicating they are long standing injuries. The fractures at the sternal ends of ribs 7 and 8 have healed with overlapping of the two fracture ends. The different stages of healing present in the ribcage indicate at least two separate traumatic events caused the rib fractures.

There is a ligamentous ossification at the site of the interosseous ligament on the distal diaphysis of the right tibia and fibula. The ossification between the two bones is interlocking but not ankylosed. This is the attachment site of the interosseous ligament and suggests a traumatic injury (Aufderheide and Rodríguez-Martín, 1998:26).

HC031

The distal diaphysis of the left femur exhibits a fusiform swelling approximately 100mm long, concentrated on the posterior of the femur at the junction of the supracondylar lines. The surface of the lesion is raised and roughened bone. There is remodelled bone formation on the anterior surface of the distal diaphysis and small raised nodules of smooth bone on the proximal third of the anterior surface of the femur. Radiographic analysis shows some occlusion of the medullary cavity.

Only the proximal thirds of all lower leg bones are present. Both tibiae have remodelled bone deposition on their diaphysis and additionally the left tibia has a partially remodelled lesion on its lateral side, adjacent to the tuberosity. Both fibulae have remodelled lesions on their diaphysis. Post depositional damage to the lower leg bones excluded the use of radiographic analysis.

Paget's disease of bone can be excluded as the characteristic radiographic appearance is absent. The sinus formation of pyogenic osteomylitis is also absent. Two diagnoses which fit the pathological changes are sclerosing osetomyelitis of Garré and treponemal disease. Sclerosing osetomyelitis of Garré is a rare disease which causes a sclerotic and fusiform thickening of the bone, which can lead to narrowing of the medullary cavity. The disease frequently effects only one bone and is often limited to one side of the diaphysis

(Aufderheide and Rodríguez-Martín, 1998). Treponemal disease may cause a periosteal bone response with a roughened outer surface, which effects only part of a bone. Later stages can see the medullary cavity totally obscured by sclerotic trabeculae (Ortner, 2003). The pathological changes are such that no definitive diagnoses can be made in this case; sclerosing osteomyelitis of Garré or treponemal disease remain the most likely causes.

There is an ossification at the lesser trochanter of the right femur possibly indicating a traumatic muscle tear of the Psoas major and/or Iliacus.

Both tibiae exhibit a Parsons' tubercle (Mays and Cooper, In press).

HC032

$M3_R$ has a protostylid.

The posterior neural arch of the atlas is cleft at the midline. The cleft is caused by a developmental delay in the growth of the two halves of the neural arch and in life the cleft would have been bridged with tough fibrous tissue (Barnes, 1994:117).

There are three small nodules of bone on the left femur around the site of the posterior cruciate ligament insertion.

There is remodelled bone formation on the anterior and lateral side of the diaphysis of the right tibia. There are similar but less well remodelled lesions on the mid-shaft of the right fibula.

There is a small oval lytic lesion approximately 10mm in length at the proximal edge of the fibular notch, on the right tibia. Radiographic analysis shows no other abnormalities.

There is extensive woven bone formation on the plural surface of the ribcage. 11 left and 10 right ribs are present, all of which are effected. Several ribs have woven bone deposits which are continuous from end to end, while others are effected along the rib in patches. The inferior surface of the sternal body also has woven bone formation on its distal half.

Bone formation on the plural surface of the rib cage has been linked to pulmonary disease. Bilateral plural rib lesions are most likely to occur in tuberculosis, however the distribution of lesions is not diagnostic of a specific infection, only pulmonary infections (Roberts and Lucy 1994, Mays *et al* 2002).

HC035

There is ossification of both acetabula labra.

There is some bone resorption on the superior margin of the articular surface of the right patella.

Both tibiae have a Parsons' tubercle (Mays and Cooper, In press).

There are areas of woven bone formation in the following locations: the posterior diaphysial surface of the left and right humeri, the shaft and distal metaphysis of both radii, the distal anterior metaphysis of both ulnae, the lateral side of the shaft of both femora (with the bone formation being more pronounced at the linea aspera), the anterior of the distal metaphysic of both femora, the shafts of both tibia (with the bone formation being more pronounced at the soleal line) and the shaft of the left fibula (the right fibula is absent). These pathological changes are consistent with a diagnosis of hypertrophic osteoarthopathy. The disease manifests with symmetrical deposits of sub-periosteal new bone formation. Tubular bones (especially those distal to the elbow and knee) are most often effected and the lesions are more prominent around areas of musculo-tendonous attachments. In modern populations inter-thoracic cancer or chronic chest infections are the most common causes of hypertrophic osteoarthopathy, although the mechanism of the bony lesions is not yet fully understood (Mays and Taylor, 2002).

HC036

The individual has a type 2 sternum (Barnes, 1994:219).

The left tibia has a Parsons' tubercle (Mays and Cooper, In press), the right tibia is absent.

There are extensive pathological changes to the right hip joint. The femoral head and neck have been completely resorbed, the lesser trochanter is present but has lost its rounded shape and become flattened. The greater trochanter is missing but post-depositional damage at the site make it impossible to ascertain the mechanism of the loss. The right femur is significantly thinner and lighter than the left femur. A small section of the acetabular rim can still be identified but the majority is obscured by new bone formation, which has completely filled the acetabulum. The edges of the lesion are partially remodelled but the centre appears to have been active at the time of death. The right innominate bone is lighter and thinner than the left and the superior and inferior pubic ramus have an elongated appearance. The loss of the articular surfaces of the femur and acetabulum have caused eburnation in the area where the two bones have made contact.

Hip dislocations (both traumatic and congenital) produce a faux joint surface, which is not seen here and can be excluded as a cause of the pathology. More probable is tuberculosis effecting the hip joint, causing destruction of the surface of both femur and acetabular surfaces. The unilateral appearance of the lesion is consistent with tuberculosis and the hip joint is the second most common area for skeletal lesions of tuberculosis to occur (Aufderheide and Rodriguez-Martin, 1998:139).

HC038

The left first metatarsal has a depressed area on the proximal articular surface.

HC043

The capitulum of the right humerus and the trochlear notch of the right ulna have small circular disturbances in their cortical bone, which have left the underlying trabecular bone exposed. The most probable cause of this lesion is osteochondritis dissicans (Aufderheide and Rodríguez-Martín, 1998:81).

There is an area of porosity on the lunate surface of both acetabula close to the superior edge of the acetabular rim.

HC049

C7 has a narrowed transverse foramen on the left and the foramen is entirely absent on the right.

The cortical surfaces of the left femur (of which only the distal half is present), the medial surface of the tibiae, the right femur and the right fibula (the left is absent) are covered in finely pitted lesions. In places this appears to be pitting of the original cortical surface but slight new bone formation is present at others. Approximately 75% of the way up the left femur, the bone shaft terminates in an area of ante-mortem destruction. The cortical walls of the diaphysis at this end are internally bevelled and have a rather rough and somewhat porous appearance. The sub-periosteal surface at the edge of this lesion has partially remodelled bone deposits. The extent of the lytic lesion on the femur is impossible to judge due to post depositional damage, but the femur head and greater trochanter are present, indicating some proximal parts of the femur were spared destruction.

The fine pitting of cortical surfaces coupled with focal destruction of the cortex from within is typical of metastatic carcinoma. The primary sites of neoplastic involvement most likely to develop skeletal metastases are the breast, kidney, lung, thyroid and prostate (Resnick & Niwayama, 1988). The prostate produces metastases which are predominantly blastic, unlike those seen here and the sex of the individual makes breast cancer unlikely. Solitary, slow growing lytic defects in long-bone shafts are most frequently caused by renal or thyroid carcinomas and so both are possible candidates for the primary

focus in the current case (Ortner, 2003: 535). However as the distribution of skeletal lesions is not predicted by the primary carcinoma no definitive diagnosis can be made (Ortner, 2003:539).

HC050

There are ligamentous ossifications on the bodies of L1 and L5.

The superior surface of the body of S1 is concave.

HC055

There is a ligamentous ossification on the body of S1.

There is thickening of the distal third of the left femoral diaphysis on the posterior aspect of the bone with an oval deposit of bone formation approximately 30mm long on the lateral diaphysis. There is remodelled bone formation covering the diaphysis of the left tibia with an area of partially remodelled bone formation on the lateral side of the proximal metaphysis. The distal diaphysis is covered with woven bone. The changes are consistent with a non-specific infection.

HC056

The underlying trabecular bone of the left mandibular condyle is almost completely exposed. The small amount of the condyle articular surface which is retained is eburnated. The molars of the left hand side of the mandible and maxilla are less worn than those on the right, suggesting that the problem with the condyle made chewing difficult on this side.

HC060

There is a benign cortical defect on the left humerus at insertion site of the teres major. Cortical defects at this position are common in sub-adults and are usually obliterated during the growth process (Mann and Murphy, 1990:85).

HC061

There is ankylosis of C6/C7/T1 and T6/T7 via large paravertebral ossification occurring at the vertebral bodies. There are several vertebrae showing similar osteophyte formation on their bodies which interlock, but are not ankylosed: T5/T6, T7/T8/T9, L2/L3. The intervertebral disc spaces have been retained and with the exception of the ossification between L2/L3 all the ossifications occur on the right hand side of the vertebral bodies. There is ossification of the costal cartilage of the manubrium and sternal body, ossification of both acetabulum labra, ossification of both glenoid labra, ossification at the site of the Achilles tendon insertion on the left calcae and ossification at the site of the insertion of

the quadriceps tendon on the right patella. The ankylosing of the vertebral bodies with retention of disk space is a classic sign of diffuse idiopathic skeletal hyperostosis (DISH). The clinical criteria for the diagnosis of DISH is that at least two complete bony bridges must be present in the spine, as is seen here (Julkunen et al, 1979).

A lumbar rib has developed on L1 indicating a caudal shift at the thoracolumbar border (Barnes, 1994:105).

L2 has some ossified disk material attached to the superior surface of the body.

There is a raised area of bone on the superior border of the lunate surface of both acetabula.

There is a raised round nodule of bone 7.3mm in diameter on the medial surface of the mandible. Radiographs show the lesion is denser than the surrounding bone and there is no evidence of communication with the dentition. The physical appearance of the lesion is consistent with an osteoma, a benign neoplasm (Steinbock, 1976:327).

The endocranial surface to the right of bregma is effected by a proliferative lesion; new bone formation carrying the impression of blood vessel channels. The majority of the right hand side of the skull is missing, due to post depositional damage so the extent of the lesion is unclear.

There is a healed fracture present on one unsided rib fragment.

HC062

C7 has formed type one cervical ribs, indicating a cranial shift at the cervicothoracic border (Barnes, 1994:100).

HC066

There is concentric fusiform thickening of the left femur centred on the junction between the middle and distal third of the shaft. The thickening is approximately 20mm long and more pronounced on the posterior surface. The surface of the lesion is of roughened cortical bone, which is most pronounced on the posterior surface. A post-depositional break at the site of the lesion reveals trabecular bone occluding the medullary cavity and radiography shows that the medullary cavity is occluded along the full length of the bone. There is a small area of roughened well-remodelled cortical bone projecting slightly from the lateral side of the left tibia, 30-40mm inferior to the fibula facet. There may be thickening of the left fibula diaphysis at this level.

The femur lesion does not seem to be consistent with a united fracture as there is no over-lapping of the bone ends, which is almost always seen in femur shaft fractures in antiquity (Aufderheide and Rodríguez-Martín, 1998:22). The lesions on the femur and tibia suggest an infectious disease and the stage of remodelling suggests lesions which were well healed and quiescent at the time of death. The involvement of two different elements suggests that if the lesions share a common cause they represent a systemic infection. Paget's disease of bone can be excluded as the characteristic radiographic appearance is absent as is the sinus formation of pyogenic osteomylitis. Two diagnoses which fit the pathological changes are sclerosing osteomyelitis of Garré and treponemal disease. Sclerosing osteomyelitis of Garré is a rare disease which causes a sclerotic and fusiform thickening of bone, leading to narrowing of the medullary cavity. The disease is usually confined to a single bone and is often limited to one side of the diaphysis (Auferheide and Rodriguez-Martín, 1998:178). Treponemal disease may cause periosteal bone response with a roughened outer surface, effecting only part of a bone with occlusion of the medullary cavity by sclerotic trabeculae (Ortner, 2003:273-297). A definitive diagnosis cannot be made in this case as the pathological changes observed are consistent with both sclerosing osteomyelitis of Garré and a treponemal infection.

There is a hole through the right illium, just inferior to the iliac crest. The main hole is 19.6mm by 7.8mm and there are two much smaller circular perforations measuring approximately 4.5mm each, just inferior to the main hole. The appearance of the lesion indicates a section of the iliac bone has fractured and has healed perpendicular to the main body of the pelvis, leaving gaps in the iliac crest. The edges of the lesion are well remodelled indicating the injury is long-standing and the position of the injury is suggestive of a downward blow to the pelvis being the cause of the fracture.

The right first metacarpal has a fracture of the articular surface of the metacarpal, commonly known as a Bennett fracture (Peterson and Bancroft, 2006).

The left innominate has a supra-acetabular cyst (Mays, 2005b).

The right acetabulum has an area of raised porous bone on the lunate surface adjacent to the acetabular rim.

HC067

There is a ligamentous ossification on the body of S1.

HC068

There is a bony outgrowth on the left distal femur at the insertion site of the adductor magnus which could indicate an injury to the muscle.

A lumbar vertebra has ossified disc material or cartilage on the superior surface of its body.

HC072

There is a lesion comprising both remodelled and active bone formation on the right distal radial metaphysis; the right ulna is not present for comparison. The lesion suggests a chronic infective condition was present.

The articular facet on the head of the first right rib is absent and the corresponding facet on the right of the vertebral body of T1 is smaller than that of the left with a deep furrow running along the inferior margin of the vertebral body facet.

T3 has a linear depression running transversely across the anterior of the superior surface of the vertebral body. Adjacent to this is an oval depression approximately 2mm deep, which has not exposed the underlying trabecular structure. The area inferior to the superior anterior rim of the body bulges outwards slightly. The appearance of the vertebra suggests a healed avulsion fracture to the vertebral body (Resnick and Niwayama.1988:2940).

HC073

The individual has a type two sternum (Barnes, 1994:219).

There is an linear depression to the endocranial surface of the left parietal bone measuring 37.3mm by 1.7mm. The right edge of the depression is straight while the left edge shows flaking of the bone; there is no sign that healing took place at the wound site. The injury is consistent with a peri-mortem blade wound; there is no evidence of the crushing effect which would have occurred if a blunter weapon was used to inflict the injury (Lovell, 1997).

HC079

There is fusiform enlargement of the right distal fibula, with a surface of roughened, well healed cortical bone. There is a remodelled periosteal reaction on the distal diaphysis of the right tibia surrounding the fibula notch. Radiographic appearance of the bone shows an oblique fracture line within the enlargement of the fibula. The morphology of the injury is consistent with a healed fracture.

The intercondylar tubercles of the right proximal tibia are superiorly elongated, rising approximately 15mm above the proximal articular surface. There is a smooth oval bony nodule approximately 10mm in length which sits proud of the articular surface anterior to the medial condyle of the right tibia.

HC080

There is a linear fracture of the left first metatarsal running anterior-posterior from the head to the proximal articular surface. The metatarsal has healed with a slight mis-alignment and the lateral side of the head sits around 2mm higher than the left. Radiographic analysis shows a fracture running through the length of the bone. The linear nature of the fracture suggests it was caused by an impact to the distal end of the first toe.

There is an interlocking non-ankylosing ligamentous ossification between the bodies of L5/S1.

There is a large circular depression on the posterior surface of the sternum between segments three and four, accompanied by medio-lateral widening of the sternum at that point. The widening suggests a delay in fusion of the sternal segments (Barnes, 1994:218).

There is remodelled new bone formation on the medial side of middle third of the diaphysis of the right tibia and a similar reaction is present on the middle third of the right fibula.

HC084

There is remodelled bone formation on the medial diaphysis of both tibiae and there is an additional raised area of woven bone formation approximately 20mm in length on the distal diaphysis of the left tibia. The surface of the lesion has the appearance of open woven bone and its lateral side is undercut. A small area of remodelled bone formation is present on the lower lateral diaphysis of the right fibula. Radiographic analysis does not show any abnormalities of the bone.

Only around 20mm of the posterior neural arch of the atlas is present extending from the right articular facet. This is a developmental defect, caused by a growth delay in the two halves of the neural arch. In life the gap in the arch would have been closed by cartilage (Barnes, 1994:117).

Type two cervical ribs have formed at C7 and T12 has taken on the facet characteristics of a lumbar vertebra. This indicates cranial shifts at the cervicothoracic and thoracolumbar borders of the spine (Barnes, 1994:100).

Post depositional damage to the frontal bone superior to the left orbit reveals replacement of diploë with abnormal nodular bone with large void spaces. The surface of the abnormal bone is irregular and fine grained. The lesion extends to the adjoining surface of the greater wing of the sphenoid and medially to the rostrum of the sphenoid body, although post depositional damage makes it impossible to gauge the extent of the lesion. There is superficial erosion of the left orbital roof and the bone there has a fine grained appearance. There is a small pitted area on the outer surface of the frontal bone, over the abnormal diploë. The lesion appears to have originated in either the diploë or

the inner table. Post depositional damage means these two possibilities cannot be distinguished. The lesion presents a mottled appearance radiographically. This is a predominantly blastic lesion originating in the diploë or inner table of the skull. The fine grained appearance of the bone is suggestive of actively expanding bone at the time of death but the dense nature of the bone when radiographed suggests a slow growing lesion. There are several possible differential diagnoses.

The frontal and parietal bones are common sites for the development of an haemangioma (Steinbock, 1976: 351). However haemangioma are lytic in nature, frequently producing a 'sunburst' effect on radiographs when present in the skull (Ortner, 2003: 513), at variance with what is observed here. Fibrous dysplasia causes the enlargement of bone by the erosion of the original cortex which is then replaced with sclerotic trabecular bone. However the gross enlargement of the bone accompanied by a thinning of cortical bone, characteristic of fibrous dysplasia are not seen in this case. Osteosarcoma is a primary malignant tumour of bone which usually occurs in those under twenty-five. The tumour is highly variable in morphology, but it is rarely found in the skull and the current case lacks the 'sunburst' appearance that is often associated with this type of tumour on X-ray (Ortner, 2003: 524). Meningiomas originate in the meningial tissue and erode through the endocranial surface often eliciting a bony reaction. They are slow growing, producing heavily ossified and well-ordered bone formation. The average age of onset for meningioma is >45 years and a recent study found that 96% of suffers were over thirty (Anderson, 1992). Of the above diagnoses, meningioma or osteosarcoma are the most likely options, although a definitive conclusion cannot be reached. The post-depositional damage obscuring the origin of the pathology eliminates a source of distinction between the two probable causes.

HC086

The individual has a type two sternum as defined by Barnes (1994:118).

HC087

There is an area of raised porous bone on the lunate surface of the right acetabulum, close to the rim.

The left transverse foramen of the atlas is divided.

HC090

There is disruption of the cortical bone on the posterior part of the lateral condyle of the left femur. The disruption is oval measuring approximately 5mm in length and exposes the underlying trabecular bone. Osteochondritis dissicans is the most likely cause of the lesion (Aufderheide and Rodríguez-Martín, 1998:81).

The lateral end of the right transverse process of L2 is present as a separate ossicle.

HC091

The left and right deciduous m2 have been retained causing a space to develop between the permanent PM2 and M1.

The lower right first molar has grossly disturbed cuspal architecture. There is a dramatic enamel hypoplasia on the buccal side of the tooth, with enamel formation ceasing 5mm from the cemento-enamel junction (cej). This leaves a gap of approximately 2mm between the edge of the buccal enamel and the occlusal surface of the tooth. The occlusal surface itself shows enamel disruption in the form of multiple small pits across its surface. The lower right PM2 also exhibits an abnormality in cusp formation and has an enamel hypoplasia 4.5mm from the cej. Disruption of the enamel also occurs in the form of pitting across the buccal surface of the tooth. The other teeth present appear normal, although wear to the anterior dental arcade may have obscured any hypoplasias present.

Mulberry molars as a result of congenital syphilis can cause a change in cuspal architecture with accompanying disruption of tooth enamel. The occlusal surface of the tooth exhibit moats of demineralisation at the base of their cusps which are not seen here and the changes in these cases are limited to the first molar (Hillson, 1998). The enamel disruption of the first molar and second premolar, coupled with the alteration in cusp organisation can be better defined as cuspal enamel hypoplasia using criteria set out by Ogden et al (2007).

Both tibiae have partially remodelled bone formation on the lateral middle third of their diaphysis.

HC093

There is an enlargement of the right middle nasal concha, measuring 20mm anterior-posterior and 15mm medio-laterally. The enlargement is teardrop shaped, with the largest anterior-posterior measurement occurring inferiorly. The surface of the enlargement is covered in tiny spicules of bone. The nasal septum deviates left so the lateral surface almost makes contact with the adjacent surface of the maxilla. Radiographic analysis shows no abnormality of the internal structure of the enlarged concha to suggest a neoplastic origin for the growth.

Modern clinical studies note that enlargement of the nasal concha is a common complaint which can result from several causes including chronic rhinitis (Berger and Gass, 2006).

The head of the right femur is displaced inferiorly so that it lies below the level of the greater trochanter. The neck is shortened, most particularly in its posterior aspect which has resulted in an abnormal posterior angulation of the head so that the fovea is more inferiorly, posteriorly orientated than normal. There appears to be callus formation beneath the head and a radiograph shows an increase in density at this area. The changes are suggestive of an impaction fracture to the femur neck.

The right acetabulum has a loss of rim height (approximately 5mm) at the superior part of the rim and the surface of the bone has become rather ragged. This lesion is suggestive of hip trauma in which a lateral impact forced the femur head against the acetabulum. The loss of rim height may suggest a minor fracture occurred during the incident but the ragged nature of the surface is more consistent with the fragmentation of the rim edge by ingress of synovial fluid (Mays 2005b). It is probable that the fracture of the femoral neck and the acetabular rim occurred at the same time.

C3 and C4 have become ankylosed at their bodies and right facet joints. C3 is laterally deviated to the right and there is no retention of intervetebral disk space. Large non-ankylosing osteophytes have formed at the vertebral bodies and right facet joints of C4, C5, and C6. There is a smooth walled concave depression on the right hand side of the bodies of C3 and C4. DISH and other arthropathies can be excluded as a cause using the criteria of Rogers and Waldron, (1995). The lateral displacement of C3 is suggests the ankylosis is secondary to a subluxation of the cervical spine (Resnick and Niwayama, 1988:2937).

There is an interlocking, non-ankylosing ligamentous ossification on the left side of the bodies of C7/T1.

HC100

There is bilateral ankylosis of the sacroiliac joints (sij), via bony bridges at the superior margins. The joint space is preserved and post depositional damage at the right sij shows that the joint surfaces are normal. There is no evidence of erosive joint lesions in the skeleton although much of the vertebral column and many of the hand and foot bones are missing. The rest of the skeleton does not exhibit bone formation due to DISH or sub-clinical DISH. The positioning of the bridging at the sij is suggestive of idiopathic fusion as described by Dar et al (2005).

HC102

There are supra-acetabular cysts in both acetabula (Mays, 2005b).

Appendix 2: Raw Data

Dentition

Maxillary Teeth

	Left								Right							
SKEL	8	7	6	5	4	3	2	1	1	2	3	4	5	6	7	8
HC005		.U	.	.D	.E	.E	.	.								
HC011	0	*	*	*	*	*	*	*	*	*	*	*	*	*	*	0
HC022	.AC4	.	.	.	.	.	.	.	.	.	.	.	.	.	.	.
HC030	0	*	*	*	.	.	.	.	.	.	.	.	*	*	.	0
HC044									X	X	X	.	.	*	.C2	X
HC056	.	.	*A	.	.	.	.	X	.	.	.	.	.	.	.	X
HC060		.U	.	.D	.D	X	X	X	X	.	X	.D	.D	.	.U	
HC061	X	*	*	*	*	*	*	*	*	*	*	*	*	*	*	.
HC062	.	.C4						X	X	.	.	.	.	.	X	.
HC066									X	.	.	.A	.A			
HC071	X	.	.	.	.	.	X	X	X	X	X	.	.	.	.	.
HC072																
HC073	.	.	.	.	.	X	X	X	X	X	.	.	.	.C5	.	.
HC084	.	.	.	.	.C4	.	.	.	.	.	.	.	.	.	.	.
HC093	X	X	X	.C4	.	.	X	X	X	X	X	XA	XA	X	*	*

Mandibular Teeth.

	Left								Right							
SKEL	8	7	6	5	4	3	2	1	1	2	3	4	5	6	7	8
HC005	0	.U	X	XD		.	.	.			.	.	.DC2	.	.U	0
HC011	*	*	*	X	.	.	.	.	.	.	.	.	X	.	.	*
HC022	.C4	*	.	.	.	.	.	.	.	.	.	.	.	*	*	.
HC030	0	.	.	.	.	.	.	.	.	.	.	.	.	.	.	0
HC032									XA	X	.	.	.	.	.	.E
HC056	.	.	.	.	X	X	X	X	X	X	X	.	.	.	.	.
HC061	*	*	*	.C4	.C2	XA	*	*	X	*	XA	.C2	.	*	*	*
HC062	.	X	X	X	X	X	X									
HC066	*	.	.AC4	.	.	.	.	.	X	.	.	.	.C2	X	.	*
HC071	X	.	.	.	.	.	.	.	.	.	.	.	.	.	.	.
HC080	0	.	*	.	.	.	.	.	.	X	X	.	.	*A	.	0
HC082				.DU	.DE	.DU	.DE	.D	.D	.DE	XD	.DE	.DU			
HC084	0	.	.	.	.	.	.	.	.	.	.	.	.	.	.	0
HC091	.E	.	*	.	X	X	.	.	.	.	.	.	.	.	.	
HC093	0	*	*	.	.	X	X	*	*	X	.	.	.	.A	*	*

Key: . = tooth present in socket, X = post mortem tooth loss, 0 = congenital absence, T = socket missing but tooth present, * = ante mortem tooth loss, A = periapical void, D = deciduous tooth, C = carie present, blank = tooth and socket missing.

Cranial Measurements

SKEL	L	B	H'	LB	MAXFRBR	GB	J	BIFRBR	S'2	S'3	S'1	biast B	FL	FB	SC	O1	O2	GL	G'H	NH'
HC011	197.0	144.0	0.0	0.0	126.0	0.0	0.0	105.8	120.7	0.0	121.9	118.0	0.0	0.0	0.0	0.0	0.0	0.0	0.0	0.0
HC022	117.0	139.0	127.0	96.0	116.0	89.6	122.7	92.7	110.6	99.7	110.0	113.0	34.2	27.9	6.6	38.1	32.0	88.9	64.0	48.4
HC030	189.0	141.0	134.0	103.0	120.0	94.0	133.8	97.0	123.1	96.8	110.3	116.3	38.2	31.2	12.6	39.3	34.1	92.7	71.1	55.6
HC061	199.0	0.0	0.0	109.0	0.0	0.0	0.0	0.0	0.0	103.2	0.0	114.8	35.3	28.1	11.6	36.3	33.1	0.0	66.0	49.2
HC062	188.0	141.0	111.0	0.0	114.2	0.0	0.0	0.0	114.1	0.0	107.7	121.4	0.0	0.0	0.0	0.0	0.0	0.0	0.0	0.0
HC066	0.0	0.0	0.0	0.0	0.0	0.0	0.0	0.0	0.0	96.4	0.0	0.0	0.0	0.0	0.0	0.0	0.0	0.0	0.0	0.0
HC068	0.0	0.0	0.0	0.0	0.0	0.0	0.0	96.4	0.0	0.0	0.0	0.0	0.0	0.0	0.0	0.0	0.0	0.0	0.0	0.0
HC071	190.0	142.0	130.0	104.0	113.0	90.5	0.0	95.2	118.9	93.7	109.9	113.5	33.3	27.5	7.4	39.7	30.2	97.1	70.7	53.1
HC073	196.0	150.0	136.0	0.0	127.0	99.7	0.0	0.0	130.1	94.4	0.0	115.2	33.6	24.2	9.9	0.0	0.0	0.0	67.0	47.9
HC080	0.0	0.0	0.0	0.0	0.0	0.0	0.0	0.0	0.0	0.0	111.4	108.5	0.0	0.0	0.0	0.0	0.0	0.0	0.0	0.0
HC084	190.0	136.0	131.0	101.1	127.0	0.0	0.0	0.0	114.1	100.6	116.3	114.3	36.5	34.3	0.0	0.0	0.0	0.0	0.0	0.0
HC093	192.0	145.0	121.0	104.0	122.0	0.0	0.0	97.6	155.5	96.0	112.1	115.4	34.0	31.2	9.0	39.5	38.0	0.0	0.0	49.6
HC100	0.0	0.0	0.0	0.0	117.8	0.0	0.0	0.0	119.1	0.0	0.0	106.0	0.0	0.0	0.0	0.0	0.0	0.0	0.0	0.0

SKEL	NB	G1	G2	DC	NH	W1	GOGO	ZZ	RB	H1	ML	CRH	CORPLEN	MANDANGLE
HC011	0.0	0.0	0.0	0.0	0.0	119.6	109.3	42.6	33.3	30.8	106.0	73.0	74.0	123
HC022	23.3	42.4	38.7	19.8	48.4	112.2	89.9	44.0	26.8	26.0	94.0	53.0	68.0	124
HC030	25.8	44.5	34.9	21.2	54.8	120.2	113.4	47.9	33.1	32.7	106.0	64.0	70.0	129
HC056	0.0	0.0	0.0	0.0	0.0	0.0	0.0	0.0	31.7	0.0	0.0	0.0	0.0	0
HC061	21.5	41.2	34.1	0.0	49.7	0.0	100.7	42.4	33.6	31.9	0.0	63.0	0.0	0
HC066	0.0	0.0	0.0	0.0	0.0	0.0	107.9	0.0	33.3	25.5	0.0	0.0	75.0	119
HC071	26.3	41.4	37.8	23.4	52.9	0.0	0.0	43.8	31.8	33.0	0.0	62.0	0.0	0
HC073	28.1	43.8	41.2	0.0	48.0	0.0	0.0	0.0	0.0	0.0	0.0	0.0	0.0	0
HC080	0.0	0.0	0.0	0.0	0.0	122.4	117.0	48.4	31.0	31.1	110.0	63.0	75.0	128
HC084	0.0	38.8	35.3	0.0	0.0	0.0	97.8	45.6	33.2	32.3	103.0	66.0	77.0	118
HC093	22.9	41.5	34.5	21.3	50.2	116.7	0.0	46.3	29.9	23.2	0.0	0.0	0.0	0

Cranial measurements are from Brothwell (1984), except for maximum frontal breadth and bi-frontal breadth, from Howells (1973).

Post-cranial Measurements

SKEL	HUMHDL	HUMMIDMAXL	HUMMIDMINL	HUMEPWL	HUMHDR	HUMMIDMAXR	HUMMIDMINR	HUMEPWR
HC003	46.3	22.5	19.6	0.0	0.0	0.0	0.0	0.0
HC005	0.0	14.0	11.9	0.0	0.0	0.0	0.0	0.0
HC006	0.0	0.0	0.0	48.9	0.0	0.0	0.0	0.0
HC010	0.0	0.0	0.0	68.3	0.0	0.0	0.0	0.0
HC011	0.0	0.0	0.0	0.0	51.0	26.4	22.4	64.2
HC014	45.4	21.3	18.6	64.9	43.8	20.6	18.3	64.7
HC016	0.0	0.0	0.0	58.2	0.0	0.0	0.0	0.0
HC022	39.2	22.6	15.8	54.9	39.9	22.1	15.1	53.6
HC023A	37.4	21.5	17.0	54.4	0.0	0.0	0.0	0.0
HC030	48.3	24.3	20.2	67.5	47.9	26.4	20.0	67.6
HC031	38.6	21.1	17.9	57.1	38.2	23.3	17.7	58.3
HC032	0.0	0.0	0.0	0.0	0.0	0.0	0.0	68.0
HC035	0.0	0.0	0.0	56.3	0.0	0.0	0.0	56.4
HC036	0.0	0.0	0.0	0.0	0.0	0.0	0.0	60.4
HC043	42.5	22.3	18.3	59.0	43.1	22.8	18.1	57.9
HC044	46.5	22.1	17.5	64.1	0.0	0.0	0.0	0.0
HC049	48.6	22.1	18.8	0.0	47.9	21.5	18.5	62.6
HC056	41.3	21.9	14.4	0.0	0.0	0.0	0.0	0.0
HC060	0.0	15.6	13.1	0.0	0.0	15.1	12.5	0.0
HC061	46.2	24.5	18.3	59.0	0.0	0.0	0.0	58.5
HC062	0.0	0.0	0.0	0.0	44.1	21.1	16.3	54.0
HC063	0.0	0.0	0.0	0.0	0.0	6.9	6.9	0.0
HC066	50.7	21.9	19.5	69.8	0.0	0.0	0.0	0.0
HC067	0.0	0.0	0.0	59.0	0.0	0.0	0.0	61.8
HC072	49.1	25.1	22.6	68.6	48.0	25.4	20.8	0.0
HC073	0.0	0.0	0.0	0.0	47.2	26.2	19.6	0.0
HC079	52.7	27.3	20.2	67.6	53.5	27.4	20.9	61.3
HC082	0.0	0.0	0.0	0.0	0.0	8.9	7.8	0.0
HC084	45.6	24.5	18.5	63.5	0.0	0.0	0.0	0.0
HC087	0.0	0.0	0.0	0.0	47.2	0.0	0.0	0.0
HC093	43.4	0.0	0.0	0.0	0.0	0.0	0.0	0.0
HC100	49.1	25.5	19.0	70.2	0.0	0.0	0.0	0.0

SKEL	FEMHDL	FEMAPL	FEMTVL	FEMMIDAPL	FEMMIDTVL	FEMBCWL	FEMHDR	FEMAPR	FEMTVR	FEMMIDAPR	FEMMIDTVR
HC001	38.2	22.3	30.9	22.8	27.2	0.0	0.0	22.8	29.3	23.3	25.4
HC003	45.9	28.1	35.9	28.3	29.4	77.4	47.0	26.8	33.2	28.8	29.7
HC005	0.0	17.0	23.1	0.0	0.0	0.0	0.0	0.0	0.0	0.0	0.0
HC006	48.1	26.7	32.4	0.0	0.0	0.0	48.3	25.8	31.7	0.0	0.0
HC010	50.5	30.5	39.2	32.1	29.6	80.2	49.2	30.7	37.2	32.3	30.0
HC013	42.7	23.9	33.7	27.3	30.0	76.1	43.3	24.6	34.2	27.1	30.0
HC014	46.3	26.5	34.7	27.5	28.2	74.4	44.4	28.0	36.0	27.8	29.2
HC016	0.0	19.5	23.9	18.6	18.4	0.0	0.0	20.3	22.6	19.5	18.2
HC017	43.4	0.0	0.0	0.0	0.0	0.0	44.5	0.0	0.0	0.0	0.0
HC020	0.0	14.4	17.5	13.1	14.3	0.0	0.0	15.4	17.6	13.0	14.4
HC022	44.9	24.2	27.9	27.1	26.0	75.9	44.2	24.6	26.5	27.2	26.9
HC025	50.6	29.0	35.8	31.6	29.0	85.5	48.9	28.9	34.8	0.0	0.0
HC026	0.0	0.0	0.0	25.6	23.8	0.0	0.0	0.0	0.0	0.0	0.0
HC030	50.2	26.9	33.3	29.2	30.0	83.7	51.3	25.1	33.6	30.0	28.8
HC031	0.0	0.0	0.0	0.0	0.0	0.0	42.4	24.1	32.5	31.9	25.9
HC032	0.0	28.0	36.5	28.7	25.2	0.0	0.0	27.2	34.4	29.6	24.0
HC035	44.3	25.2	34.6	28.4	29.2	74.3	44.9	26.2	31.9	28.3	28.4
HC036	45.0	28.6	33.1	31.1	26.4	0.0	28.9	16.2	0.0	0.0	0.0
HC043	43.6	25.9	31.0	32.3	26.0	74.2	43.0	26.2	31.0	29.1	24.9
HC045	0.0	13.5	15.3	11.6	13.4	0.0	0.0	13.8	15.4	11.7	13.2
HC050	44.0	27.3	32.7	0.0	0.0	74.9	0.0	0.0	0.0	0.0	0.0
HC055	47.0	27.1	34.3	28.9	30.1	0.0	0.0	0.0	0.0	0.0	0.0
HC060	0.0	16.9	22.1	17.1	16.8	0.0	0.0	17.8	20.9	17.1	16.3

HC061	43.6	27.3	31.3	28.2	27.6	77.5	44.2	27.4	30.0	30.4	26.1
HC062	43.3	22.3	31.3	25.3	27.3	70.6	43.5	23.8	30.9	25.7	25.9
HC066	55.5	28.6	38.0	36.3	32.2	89.0	55.9	28.4	37.3	0.0	0.0
HC067	45.3	24.8	32.3	0.0	0.0	0.0	45.3	23.5	31.4	0.0	0.0
HC071	49.6	29.6	33.6	29.9	28.5	79.8	49.5	28.8	34.2	29.3	28.3
HC079	55.6	32.8	33.8	36.2	30.1	79.6	51.8	30.7	35.6	34.8	29.7
HC080	49.7	27.4	33.6	35.9	27.8	0.0	49.3	29.5	33.8	27.9	0.0
HC084	50.7	29.0	31.4	33.1	28.0	78.2	0.0	0.0	0.0	0.0	0.0
HC086	0.0	0.0	0.0	0.0	0.0	0.0	0.0	25.5	29.6	25.9	24.3
HC087	46.1	0.0	0.0	28.4	30.0	81.3	46.8	26.6	33.9	28.1	29.6
HC088	39.1	23.3	28.7	21.2	23.5	66.1	37.7	25.4	27.1	24.1	22.4
HC090	0.0	24.1	38.2	28.5	31.7	80.7	0.0	0.0	0.0	0.0	0.0
HC091	0.0	0.0	0.0	0.0	0.0	0.0	0.0	28.5	30.0	29.1	25.5
HC093	0.0	0.0	0.0	0.0	0.0	0.0	44.6	26.4	28.5	27.4	24.8
HC100	0.0	0.0	0.0	0.0	0.0	0.0	0.0	29.0	37.6	0.0	0.0

SKEL	FEMBCWR	TIBAPL	TIBTVL	TIBAPR	TIBTVR	FEMLENL	FEMLENR	TIBLENL	TIBLENR	FIBLENL	FIBLENR
HC001	0.0	28.3	21.8	29.3	22.2	408	408	0	334	0	0
HC003	76.5	34.2	22.4	34.1	22.5	435	436	355	352	346	336
HC010	80.9	38.1	26.4	38.2	27.5	468	468	0	0	0	0
HC013	76.3	29.5	24.5	0.0	0.0	419	414	0	0	0	0
HC014	76.4	34.6	24.7	35.4	24.4	447	445	346	348	343	341
HC015	0.0	36.8	27.4	38.1	27.1	0	0	0	0	0	0
HC016	0.0	22.4	19.9	23.1	19.9	300	300	0	229	221	0
HC017	0.0	0.0	0.0	0.0	0.0	419	420	340	0	334	0
HC020	0.0	15.2	12.7	14.9	12.7	199	199	159	158	0	155
HC022	75.0	27.6	22.8	27.5	22.4	441	444	338	332	342	0
HC025	0.0	39.8	25.7	40.0	26.6	473	0	375	368	0	0
HC026	0.0	30.9	24.2	30.8	23.7	403	0	311	309	0	0
HC030	82.5	34.7	27.3	35.4	27.8	445	445	346	347	341	342
HC031	75.3	32.6	23.0	33.0	24.2	0	438	0	0	0	0
HC035	73.8	34.5	23.4	34.7	23.6	430	432	368	362	0	0
HC036	71.3	33.6	22.9	0.0	0.0	417	0	349	0	0	0
HC038	0.0	0.0	0.0	32.9	25.4	0	0	0	376	0	0
HC043	74.6	33.7	24.8	33.2	24.6	467	469	0	402	0	0
HC045	0.0	14.8	13.3	14.2	13.7	149	151	120	118	115	0
HC049	0.0	32.4	22.2	31.9	22.2	0	0	350	0	0	0
HC050B	0.0	0.0	0.0	0.0	0.0	0	181	0	0	0	0
HC055	0.0	0.0	0.0	0.0	0.0	453	0	0	0	0	0
HC060	0.0	21.0	15.8	22.2	16.3	243	243	202	201	195	194
HC061	77.5	35.9	24.8	35.4	24.5	414	413	0	334	333	331
HC062	71.9	29.3	22.1	28.5	22.9	415	415	327	326	0	0
HC066	0.0	41.6	25.9	41.1	27.0	492	0	0	0	0	0
HC068	0.0	35.0	21.6	34.9	21.5	0	0	0	0	0	0
HC071	78.0	33.8	25.8	36.2	25.6	464	463	367	364	0	0
HC079	83.9	42.3	27.3	40.6	26.7	513	508	420	422	0	0
HC080	0.0	34.5	25.3	0.0	27.6	460	461	384	375	0	0
HC084	0.0	36.5	25.4	35.8	27.3	459	0	356	361	350	348
HC086	0.0	0.0	0.0	0.0	0.0	0	428	0	0	0	0
HC087	81.8	0.0	0.0	32.2	23.1	430	426	0	367	0	357
HC088	67.0	27.1	20.2	26.2	20.8	407	400	336	335	0	334
HC090	0.0	0.0	0.0	0.0	0.0	481	0	0	0	0	0
HC091	0.0	33.5	26.6	34.5	27.6	0	413	333	323	0	325
HC093	77.5	0.0	0.0	31.0	25.5	0	422	0	0	0	0

SKEL	HUMLENL	HUMLENR	RADLENL	RADLENR	ULNALENL	ULNALENR	CLAVLENL	CLAVLENR
HC001	0.0	0.0	0.0	224.0	0.0	244.0	126.0	0.0
HC003	316.0	0.0	0.0	0.0	0.0	0.0	0.0	0.0
HC005	210.0	0.0	0.0	157.0	177.0	0.0	0.0	0.0
HC010	0.0	0.0	244.0	0.0	269.0	0.0	144.0	0.0
HC011	0.0	337.0	0.0	0.0	0.0	0.0	0.0	0.0
HC013	0.0	0.0	0.0	0.0	245.0	0.0	0.0	0.0
HC014	311.0	314.0	231.0	233.0	249.0	250.0	143.0	138.0
HC016	0.0	0.0	161.0	162.0	172.0	178.0	0.0	0.0
HC020	0.0	0.0	115.0	0.0	128.0	0.0	0.0	0.0
HC022	309.0	304.0	224.0	224.0	245.0	243.0	127.0	129.0
HC023A	295.0	0.0	211.0	0.0	232.0	0.0	0.0	0.0
HC025	0.0	0.0	250.0	0.0	272.0	0.0	0.0	0.0
HC030	319.0	321.0	238.0	237.0	259.0	257.0	142.0	0.0
HC031	313.0	315.0	230.0	233.0	0.0	0.0	134.0	0.0
HC032	0.0	0.0	0.0	0.0	0.0	0.0	140.0	141.0
HC035	0.0	0.0	244.0	0.0	264.0	0.0	0.0	0.0
HC043	339.0	345.0	250.0	255.0	264.0	271.0	148.0	0.0
HC044	0.0	338.0	0.0	0.0	0.0	0.0	0.0	0.0
HC045	0.0	0.0	86.0	86.0	96.0	96.0	0.0	0.0
HC049	327.0	330.0	0.0	248.0	0.0	265.0	0.0	0.0
HC050B	141.0	0.0	107.0	0.0	114.0	0.0	0.0	0.0
HC056	287.0	0.0	0.0	0.0	0.0	0.0	0.0	0.0
HC060	171.0	173.0	132.0	0.0	150.0	151.0	88.0	0.0
HC061	300.0	0.0	218.0	0.0	0.0	0.0	142.0	0.0
HC062	0.0	312.0	216.0	222.0	0.0	0.0	0.0	0.0
HC063	0.0	72.0	0.0	0.0	0.0	0.0	0.0	0.0
HC066	349.0	0.0	0.0	0.0	0.0	0.0	152.0	0.0
HC067	0.0	0.0	0.0	0.0	244.0	0.0	0.0	0.0
HC072	325.0	329.0	0.0	0.0	0.0	0.0	153.0	0.0
HC073	0.0	340.0	0.0	248.0	0.0	266.0	153.0	0.0
HC079	367.0	360.0	0.0	0.0	0.0	0.0	155.0	157.0
HC082	0.0	102.0	0.0	0.0	0.0	0.0	0.0	56.0
HC084	324.0	0.0	235.0	0.0	258.0	0.0	157.0	152.0
HC086	0.0	0.0	0.0	0.0	0.0	0.0	143.0	0.0
HC087	0.0	0.0	0.0	242.0	0.0	0.0	0.0	0.0
HC088	0.0	0.0	207.0	0.0	225.0	231.0	0.0	0.0
HC090	0.0	0.0	261.0	260.0	0.0	0.0	0.0	0.0
HC091	0.0	0.0	214.0	0.0	0.0	0.0	0.0	138.0
HC093	0.0	0.0	0.0	223.0	0.0	240.0	134.0	0.0
HC100	333.0	0.0	0.0	0.0	0.0	0.0	0.0	0.0

Cranial non-metrics

SKEL	1	2	3	4	5	6	7	8	9	10	11	12	13	14	15	16	17	18	19	20	21	22	23	24	25	26	27	28	29	30	31	32	33	34
HC001												0/-	0/-											1/-										
HC003												0/-	0/-																					
HC005	0	1	1	0								0/0	0/0				0				0/0		0/1	1/-	1/0	1/1	0/0		1/-	0/0	1/-	1/1	0	0/0
HC006												0/-	0/-											-/1										
HC011	0	0		0		0		0/-			0/0	0/0	0/0	1/0					0/0	1/0	0/-	1/1	0/0	0/0	1/-	0/-	1/-					0/0		1/1
HC022	0	0	1	0	0	0	0	0/0	0/0	0/0	0/0	0/0	0/0	0/0	0/0	0/0	0	0	1/1	0/0	0/0	0/0	0/0	1/1	0/1	1/1	0/0	0/0	0/0	0/0	0/0	0/0	0	0/0
HC030	0	0	0	0		0	1			0/-	0/0	0/0	1/0	0/0	0/0	0/0	0	0	1/1	0/0	0/0	0/0	1/1	1/1	0/0	0/0	0/0	0/0	0/0	1/1	0/0	0/0	0	0/0
HC032												-/0	-/0								0/-	1/-			0/-							0/0		-/0
HC056	1	0										-/0	-/0				0	0					0/-	-/1						0/0	0/0	0/0	0	0/0
HC060	0	0		0								-/0	-/0				0	0				1/1	0/1	1/1					0/-	0/0	0/0	-/0	0	-/0
HC061	0	0	1	0	0		0		0/-	0/-	0/-	0/0	0/-	0/-		0/0	0	0	0/-	0/-	0/0	0/0	0/0	0/-	1/1	0/1	0/0	0/0	1/1	0/-	0/0	0/0	0	0/0
HC062	0	0	0	0	0	0	0				0/0	0/0	0/0	0/0			0		0/0	1/1	0/0	1/1	-/0	-/1	0/0		0/0	0/0	0/0	-/1	0/0	0/0		
HC066	0	1	1	0		0						0/0	0/0						1/-		-/0	0/0		0/-	-/0	-/0	-/0	-/0				0/0	0	0/0
HC068	0	0		0		0																0/0		-/1										
HC071	0	0	0	0	0	0	0	0/0	0/0	0/0	0/0	0/0	0/0	0/0		0/0	0	0	-/0	-/0	0/0	1/1	1/0	0/0	0/0	0/0	0/0	0/0	0/0	0/0	0/0	0/0	0	-/0
HC073	0	0	1	0	0	0	0	0/-	0/-	0/0	-/0	0/0	0/1	-/0			0	0	-/0	-/0	0/0	0/1	0/0	1/1	0/0	0/1	0/0	0/0	-/1	0/0	0/0			
HC080	0			0								-/0	-/0																	0/-		1/1	0	0/0
HC084	0	0	1	0		0	1	-/0	-/0	-/0	0/1	0/0	0/0	1/0	-/0		0	0			0/0	0/1	1/1	1/1		1/0	0/0	-/0	0/1	0/0	0/0	1/1	0	0/0
HC093	0	0	1	0		0	0	-/0	-/1	-/0	-/0	0/0	0/0	0/0		-/0	1	0	1/1	0/0	0/0	1/0	0/0	1/-	0/0	0/0	0/0	0/0	0/0	1/0	0/0	0/0	0	0/0
HC100	0	0	0	0	0	0	0					0/0	0/0									1/1		-/1						0/-				

Key: 1= metopic suture, 2= ossicle at lambda, 3= lambdoid ossicle, 4= inca bone, 5= sagittal ossicle, 6= ossicle at bregma, 7= coronal ossicle, 8= fronto-temporal articulation, 9= epipteric bone, 10= squamo-parietal ossicle, 11= auditory torus, 12= foramen of Hushke, 13= ossicle at asterion, 14= clinoid bridging, 15= pterygoid bridging, 16= palatine torus, 17= maxillary torus, 18= mastoid foramen extra-sutural, 19= mastoid foramen absent, 20= double condylar facet on occipital, 21= parietal foramen, 22= accessory infra-orbital foramen, 23= zygomatic facial foramen, 24 divided hypoglossal canal, 25= posterior condylar canal patent, 26= precondylar tubercle, 27= foramen ovale incomplete, 28= accessory lesser palatine foramen, 29= supra-orbital foramen complete, 30= maxillary M3 absent, 31= mandibular M3 torus, 32= mandibular torus, 33= mylohyoid bridging. Blank= element not present for observation, 0= trait absent, 1= trait present. Bi-lateral traits are scored left/right.

Post cranial non-metrics.

SKEL	1	2	3	4	5	6	7	8	9	10	11	12	13	14	15	16	17	18	19	20	21	22	23
HC001	1/1	0/0	0/0		-/0		1/1	0/0	0	1							0/0	1/0	0/0	0/0			
HC003	0/0	0/0	1/1	1/1	0/-	0/-								0/0	0/0	0/0	0/0	0/1	0/0	0/0			
HC005	1/-							0/-													0/0	0/0	0/0
HC006	1/1	0/0	0/0	0/0	0/-	0/-	0/0	1/0	0	0													
HC010	0/0	0/0	1/1	0/1	0/-	0/-	0/0	1/1	0	1	0/-	0/-	0/-										
HC011					-/0	-/0					-/0	-/0									0/0	0/0	0/0
HC013	0/0	0/0	0/0	1/1					0	0								-/1					
HC014	1/1	0/0	1/1	0/0	0/0	0/0	0/0	0/0	0	0	0/0	0/0	-/0	-/0	-/0	-/0	0/0	0/0	0/0	0/0	0/0	1/0	0/1
HC016	1/1				0/-	0/-			0	0													
HC017	-/0	0/0	-/0	0/0				-/0	0	0				1/1	0/0	0/0	0/0	1/1	-/1	-/0			
HC020	1/1	0/0	0/0		0/0	0/0		0/0					0/0						0/0	0/0			
HC022	0/0	0/0	0/0	0/0	0/0	0/0	0/0	0/0	0	1	0/0	0/0	0/0	0/-	0/-	0/-	0/0	1/1	1/1	0/0	0/0	0/0	0/0
HC023A					0/-	0/-					0/-	0/-											
HC023B								0/-	0	0													
HC025	0/0	1/1	0/0	1/-			0/0	1/1	0	1				0/0	0/0	0/0	1/1	1/0	0/0	0/0			
HC026	0/0													-/0	-/0	-/0			1/1	0/0			
HC030	0/0	0/0	1/1	0/0	0/0	0/0	0/0	1/1	0	0	0/0	1/0	0/0	-/0	-/0	-/0	0/0	1/1	0/0	0/0	0/0	0/1	0/0
HC031	0/0	0/0	0/0	1/0	0/0	0/1	1/1	1/1	0	1		0/-											
HC032	1/1	0/0	0/0	0/0	-/0	0/0	0/-	0/-	0	0			-/0						-/0	-/0	0/0	0/0	0/0
HC035	0/0	0/0	1/1	1/1	0/0	0/0	0/0	1/1						-/0	-/0	-/0	0/0	0/1	-/1	-/0			
HC036	0/-	0/-	0/-	0/-	-/0	-/0	0/-	0/0	0	0							0/-	1/-					
HC038														-/0	-/0	-/0	-/0	-/0	0/0	0/0			
HC040								-/1	0	0			0/-								0/0	0/0	0/0
HC043	0/0	0/0	0/0	1/1	0/0	1/-	0/0	1/1	0	1	0/0	0/0	0/-					-/0	1/-	0/-	0/0	0/0	0/0
HC044					0/-	0/-					0/-	0/-											
HC045	1/1	0/0	0/0		-/0	-/0		0/0															
HC049					1/0	0/0		0/0	0	0				-/0	-/0	-/0	0/-						
HC050	1/0	0/0	0/0	1/1	-/0	-/1	1/1	1/0	0	1													

SKEL	1	2	3	4	5	6	7	8	9	10	11	12	13	14	15	16	17	18	19	20	21	22	23
HC055	0/-	0/-	1/-	0/-					0	1													
HC056					0/-	0/-															0/0	0/0	0/0
HC060	1/1	0/0	0/0		0/0		0/0	0/0		0	-/0	-/0	0/0						0/-	0/-	0/0	-/0	-/0
SKEL	1	2	3	4	5	6	7	8	9	10	11	12	13	14	15	16	17	18	19	20	21	22	23
HC061	0/0	0/0	0/1	1/1	0/0	0/0	1/1	0/0	0	1	0/0	0/0	0/0	1/1	0/0	0/0	0/0	1/1	0/0	0/0	1/1	0/0	0/0
HC062	1/0	0/0	0/0	1	0/0	0/1	0/0	0/0	0	0				0/0	0/0	0/0	0/0	0/0	0/0	0/0	0/0	0/0	0/0
HC066	0/0	0/1	0/0	1/-	0/0	0/0	0/0	0/0									-/0				0/0	0/0	
HC067	0/0	0/0	1/1	0/0	0/0	0/0	0/0	0/0	0	0													
HC068					0/-		0/0	-/0		0							0/-	1/-					
HC071	0/0	0/0	0/0	1/0	0/0	0/0	0/0	0/0	0	1							0/0	0/0	1/1	0/0	1/-		0/-
HC072					0/0	0/0					0/-	0/-											
HC073					-/1	-/0					0/0	0/0	0/0								1/1	0/0	0/0
HC079	0/0	0/-	1/1	0/0	0/0	0/0	-/0				0/0	0/0		-/0	-/0	-/0	0/0	0/0	1/1	0/0			
HC080	0/0	0/0	1/1	0/-	0/0	0/0	0/0		0	0							0/-	1/-	0/-	0/-	0/-	0/-	0/-
HC084	1/-	0/-	0/-	1/-	0/-	0/-	0/-	0/-	0	0	0/-	0/-	0/-				0/0	1/1			0/0	0/0	0/0
HC086							-/0			1													
HC087	-/0	-/0	-/1		0/0		0/0							0/0			-/0	-/0	0/-	0/-	0/0	0/0	0/0
HC088	1/1	0/0	0/0	0/0			1/0	0/0	0	0							0/0	0/1					
HC090	1/-	0/-	0/-	1/-			0/-	0/-															
HC091	-/0	-/0	-/0	-/0	0/-	0/-		-/0	0	0											0/0	0/0	1/0
HC093				-/1																	0/0	0/0	0/0
HC100	-/0	-/0	-/0	-/1	0/-	0/-	0/0		0														
HC102	0/-	0/-	1/-	1/-			0/-										-/0	-/0	-/0	-/0			

Key: 1= Fossa of Allen, 2= Poirier's facet, 3= plaque formation, 4= exostosis in trochanteric fossa, 5= supra-condylar process, 6= septal aperture, 7= acetabular crease, 8= accessory sacral facets on ilium, 9= spina bifida, 10= sacralisation of L5, 11= acromial articular facet, 12= os acromiale, 13= supra-scapula foramen, 14= vastus notch, 15= vastus fossa, 16= emarginated patella, 17= medial squatting facets, 18= lateral squatting facets, 19= anterior calcaneal facet double, 20= anterior calcaneal facet absent, 21= atlas facet double, 22= posterior bridging, 23= lateral bridging. Blank= no element present for observation, 0= trait absent, 1= trait present. Bi lateral traits are scored left/right.

Cribra orbitalia, Calculus and Enamel Hypoplasias

SKEL	CRIBRA	CALC	DENTAL ENAMEL HYPOPLASIA
HC005		0	0
HC011	0	3	0
HC022	0	1	2 BANDS ON I1 LOWER RIGHT 6.5 AND 7.0MM CEJ
HC030	C	2	ONE LINE ON UPPER RIGHT I1 AT 4MM CEJ
HC032		0	
HC056	0	3	0
HC061	0		
HC062	0	1	0
HC066		2	TWO LINES AT 2.5MM AND 3.7MM CEJ ON PM1 BOTTOM R
HC068	0	1	0
HC071	C	1	0
HC073		1	
HC080	C	2	0
HC084		1	
HC091		2	ONE LINE ON LOWER RIGHT CANINE AT 11.1MM CEJ ONE LINE ON LOWER RIGHT PREMOLAR 5MM CEJ
HC093	0	0	0

Key: Cribra – Blank= orbits absent, 0= orbits normal, C=cribrotic, P=porotic (Brothwell, 1981). Calculus is scored from Dobney and Brothwell (1987).

Spinal Osteoarthritis

		Cervical					Thoracic					Lumbar			
SKEL		0	1	2	3		0	1	2	3		0	1	2	3
HC001		0	0	0	0		7	0	0	0		3	0	0	0
HC005		7	0	0	0		0	9	0	0		3	0	0	0
HC010		0	0	0	0		7	2	2	0		3	0	2	0
HC011		0	1	2	4		4	0	0	2		0	0	0	0
HC013		0	0	0	0		0	1	0	0		2	0	2	0
HC014		7	0	0	0		7	1	3	0		6	0	0	0
HC016		0	0	0	0		4	0	0	0		5	0	0	0
HC017		0	0	0	0		0	0	0	0		2	0	0	0
HC017B		1	0	0	0		5	0	0	0		1	0	0	0
HC020		0	0	0	0		12	0	0	0		5	0	0	0
HC022		7	0	0	0		12	0	0	0		5	0	0	0
HC023B		0	0	0	0		2	0	1	0		4	1	0	0
HC025		0	0	0	0		3	0	1	0		1	2	2	0
HC030		3	0	0	4		10	0	0	2		2	3	1	0
HC031		3	3	0	0		7	0	5	0		2	1	2	0
HC032		6	0	0	0		12	0	0	0		5	0	0	0
HC035		0	0	0	0		5	0	0	0		5	0	0	0
HC036		0	0	0	0		6	0	0	0		5	0	0	0
HC040		3	1	0	1		8	2	0	1		5	0	0	0
HC043		0	2	2	2		6	1	4	1		1	3	0	0
HC044		0	0	0	0		8	0	0	1		1	0	0	0
HC045		1	0	0	0		5	0	0	0		3	0	0	0
HC049		1	0	0	0		11	0	0	0		5	0	0	0
HC050		0	0	0	0		0	0	0	0		2	1	0	2

		Cervical					Thoracic					Lumbar			
SKEL		0	1	2	3		0	1	2	3		0	1	2	3
HC050B		7	0	0	0		3	0	0	0		3	0	0	0
HC056		1	0	0	1		9	0	0	0		2	0	0	0
HC060		6	0	0	0		7	0	0	0		5	0	0	0
HC062		4	1	2	0		8	2	2	0		4	0	1	0
HC066		2	5	0	0		9	1	0	0		5	0	0	0
HC067		2	0	0	0		7	4	0	0		4	0	0	1
HC068		0	0	0	0		0	0	0	0		2	0	0	0
HC071		5	0	0	0		8	2	0	0		5	0	0	0
HC072		0	0	0	0		9	1	0	0		0	0	0	0
HC073		7	0	0	0		12	0	0	0		1	0	0	0
HC079		0	0	0	0		0	0	0	1		0	0	0	0
HC080		2	0	0	0		12	0	0	0		5	0	0	0
HC082		3	0	0	0		8	0	0	0		3	0	0	0
HC084		4	0	0	0		12	0	0	0		5	0	0	0
HC086		0	0	0	0		9	0	0	0		5	0	0	0
HC087		0	2	0	0		0	0	0	0		1	1	0	0
HC088		2	0	0	0		0	0	0	0		5	0	0	0
HC090		0	0	0	0		0	0	0	0		2	0	0	0
HC091		7	0	0	0		9	0	0	0		5	0	0	0
HC093		2	0	2	2		6	0	2	0		1	3	0	0
HC100		0	0	0	0		0	0	0	0		4	0	0	0

Spinal Osteoarthritis

		Cervical				Thoracic				Lumbar			
SKEL	0	1	2	3	0	1	2	3	0	1	2	3	OPS1
HC001	0	0	0	0	7	3	0	0	1	3	0	0	
HC005	6	0	0	0	9	0	0	0	3	0	0	0	
HC010	0	0	0	0	4	6	0	0	2	2	1	0	0
HC011	0	1	2	3	0	4	2	0	0	0	0	0	
HC014	4	2	0	0	7	4	0	0	0	6	0	0	0
HC016	0	0	0	0	4	0	0	0	5	0	0	0	0
HC017	0	0	0	0	0	0	0	0	2	0	0	0	0
HC017B	0	0	0	0	5	0	0	0	1	0	0	0	0
HC020	0	0	0	0	12	0	0	0	5	0	0	0	
HC022	5	0	0	0	12	0	0	0	5	0	0	0	0
HC023B	0	0	0	0	1	1	0	0	1	1	0	0	0
HC025	0	0	0	0	1	0	0	0	3	2	1	0	0
HC030	1	0	0	5	4	8	0	0	0	3	3	0	1
HC031	2	4	0	0	1	6	5	0	0	2	3	0	1
HC032	5	0	0	0	12	0	0	0	5	0	0	0	0
HC035	0	0	0	0	5	0	0	0	5	0	0	0	
HC036	0	0	0	0	6	0	0	0	2	3	0	0	0
HC040	4	0	0	0	3	3	1	0	3	1	1	0	0
HC043	3	0	2	0	3	1	8	0	2	1	0	1	3
HC044	0	0	0	0	2	0	0	0	0	0	0	0	
HC045	1	0	0	0	5	0	0	0	3	0	0	0	0
HC049	1	0	0	0	11	0	0	0	5	0	0	0	0
HC050	0	0	0	0	0	0	0	0	1	3	1	0	0
HC050B	6	0	0	0	3	0	0	0	3	0	0	0	
HC056	0	0	1	0	5	0	0	0	0	0	0	0	

	Cervical				Thoracic				Lumbar				
SKEL	0	1	2	3	0	1	2	3	0	1	2	3	OPS1
HC062	5	1	0	0	5	7	0	0	0	5	0	0	0
HC066	2	2	2	0	3	6	0	0	0	3	1	0	0
HC067	1	1	0	0	4	7	0	0	2	3	0	0	0
HC068	0	0	0	0	0	1	4	0	0	4	1	0	0
HC071	4	0	0	0	10	0	0	0	5	0	0	0	0
HC072	0	0	0	0	5	7	0	0	0	0	0	0	
HC073	6	0	0	0	12	0	0	0	1	0	0	0	
HC079	0	0	0	0	0	1	0	0	0	1	1	0	0
HC080	0	0	0	0	5	6	0	0	4	1	0	0	
HC082	2	0	0	0	8	0	0	0	3	0	0	0	
HC084	3	0	0	0	12	0	0	0	5	0	0	0	
HC086	0	0	0	0	9	0	0	0	5	0	0	0	0
HC087	1	0	0	0	0	0	0	0	0	2	0	0	
HC088	2	0	0	0	0	0	0	0	5	0	0	0	0
HC090	0	0	0	0	0	0	0	0	2	0	0	0	
HC091	6	0	0	0	11	0	0	0	5	0	0	0	
HC093	0	0	0	5	2	9	1	0	0	1	4	0	0
HC100	0	0	0	0	0	0	0	0	4	0	0	0	

Osteoarthritis

SKEL	GR1OA	GR2OA	GR3OA
HC001	2L RIBS		
HC003	R PATELLA		
HC010	3L RIBS 3R RIBS	2L RIBS	1U HPHALANX
HC011	D RHUMERUS R GLENOID	LAT RCLAVICLE	
HC014	1L RIB 2R RIBS D RFEMUR		
HC023B	S1		
HC030		LAT RCLAVICLE LAT LCLAVICLE 3R RIBS 4L RIBS	3R RIBS 1L RIB S1 R GLENOID
HC031	2L RIBS 2R RIBS		
HC035	P LULNA P RULNA P LRADIUS D LFEMUR D RFEMUR R PATELLA		
HC036	1R RIB D LFEMUR	2R RIBS S1	1L RIB 2R RIBS
HC040	2L RIBS 2R RIBS	2L RIBS	
HC043	1L RIB 2R RIBS	2L RIBS MED RCLAVICLE S1	
HC044	1L RIB		
HC056		6L RIBS 4R RIBS	LMC
HC061	3L RIBS 4R RIBS P RTIBIA D RFEMUR L GLENOID R GLENOID	1L RIB MED LCLAVICLE MED RCLAVICLE LAT LCLAVICLE LAT RCLAVICLE	1R RIB D LRADIUS R1ST PROX HAND PHALANX DIST END
HC062	2L RIBS 3R RIBS	1L RIB 4R RIBS S1	
HC066	3L RIBS 4R RIBS D LFEMUR P LULNA P RULNA D RULNA	1L RIB LAT LCLAVICLE LAT RCLAVICLE	
HC067	2L RIBS 1R RIB	1R RIB	
HC068	1R RIB		
HC071	1L RIB 1R RIB		
HC072	3L RIBS 4R RIBS	1L RIB 1R RIB	
HC073	1L RIB		
HC079	D RHUMERUS P LULNA P RULNA L GLENOID R GLENOID D LFEMUR R PATELLA 1L MC3	LAT LCLAVICLE LAT RCLAVICLE	L ACETABULUM D LHUMERUS P LRADIUS D RFEMUR P LFEMUR 1L MC1
HC084	1R RIB		
HC088	1L RIB		
HC093	2L RIBS 1R RIB	S1 LAT LCLAVICLE	LMC
HC102			1L MT


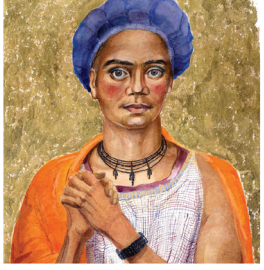



ENGLISH HERITAGE RESEARCH DEPARTMENT

English Heritage undertakes and commissions research into the historic environment, and the issues that affect its condition and survival, in order to provide the understanding necessary for informed policy and decision making, for sustainable management, and to promote the widest access, appreciation and enjoyment of our heritage.

The Research Department provides English Heritage with this capacity in the fields of buildings history, archaeology, and landscape history. It brings together seven teams with complementary investigative and analytical skills to provide integrated research expertise across the range of the historic environment. These are:

* *Aerial Survey and Investigation*
* *Archaeological Projects (excavation)*
* *Archaeological Science*
* *Archaeological Survey and Investigation (landscape analysis)*
* *Architectural Investigation*
* *Imaging, Graphics and Survey (including measured and metric survey, and photography)*
* *Survey of London*

The Research Department undertakes a wide range of investigative and analytical projects, and provides quality assurance and management support for externally-commissioned research. We aim for innovative work of the highest quality which will set agendas and standards for the historic environment sector. In support of this, and to build capacity and promote best practice in the sector, we also publish guidance and provide advice and training. We support outreach and education activities and build these in to our projects and programmes wherever possible.

We make the results of our work available through the Research Department Report Series, and through journal publications and monographs. Our publication Research News, which appears three times a year, aims to keep our partners within and outside English Heritage up-to-date with our projects and activities. A full list of Research Department Reports, with abstracts and information on how to obtain copies, may be found on www.english-heritage.org.uk/researchreports

For further information visit www.english-heritage.org.uk

ENGLISH HERITAGE